

VISVESVARAYA TECHNOLOGICAL UNIVERSITY

JNANA SANGAMA, BELAGAVI - 590018



A Project Report on

**Design and Development of an H-Frame Drone for Cleaning
Solar Panels and High-Rise Buildings**

Submitted in partial fulfilment of the requirements for the award of the degree of

Bachelor of Engineering

in

Electronics and Communication Engineering

for the Academic Year: 2024-25

Submitted by

Chaya R (1NT21EC037)

Mohit Mohan (1NT21EC085)

Venu V Muthyala (1NT21EC169)

Under the Guidance of

Dr. Murthy M

Assistant Professor

Dept. of Electronics and Communication Engineering



NITTE
EDUCATION TRUST

**NITTE MEENAKSHI
INSTITUTE OF TECHNOLOGY**

VISVESVARAYA TECHNOLOGICAL UNIVERSITY

JNANA SANGAMA, BELAGAVI - 590018



A Project Report on

**Design and Development of an H-Frame Drone for Cleaning Solar
Panels and High-Rise Buildings**

Submitted in partial fulfilment of the requirements for the award of the degree of

Bachelor of Engineering

in

Electronics and Communication Engineering

for the Academic Year: 2024-25

Submitted by

Chaya R (1NT21EC037)

Mohit Mohan (1NT21EC085)

Venu V Muthyala (1NT21EC169)

Under the Guidance of

Dr. Murthy M

Assistant Professor

Dept. of Electronics and Communication Engineering



NITTE
EDUCATION TRUST

**NITTE MEENAKSHI
INSTITUTE OF TECHNOLOGY**

An Autonomous Institution Affiliated to VTU

DEPARTMENT OF ELECTRONICS AND COMMUNICATION ENGINEERING

YELAHANKA, BENGALURU- 560064

DEPARTMENT OF ELECTRONICS AND COMMUNICATION ENGINEERING
BENGALURU- 560 064

Certificate

Certified that the project work titled “**Design and Development of an H-Frame Drone for Cleaning Solar Panels and High-Rise Buildings**” is carried out by **Chaya R (INT21EC037)**, **Mohit Mohan (INT21EC085)**, and **Venu V Muthyala (INT21EC169)**, Bonafide students of Nitte Meenakshi Institute of Technology in partial fulfilment for the award of Bachelor of Engineering in Electronics and Communication Engineering of Visvesvaraya Technological University, Belagavi during the academic year 2024-2025. The project report has been approved as it satisfies the academic requirement in respect of the project work prescribed as per the autonomous scheme of Nitte Meenakshi Institute of Technology for the said degree.

Signature of the Guide

Dr. Murthy M
Assistant Professor
Dept. of ECE, NMIT

Signature of the HOD

Dr. Parameshachari B D
HOD
Dept. of ECE, NMIT

Signature of the Principal

Dr. H C Nagaraj
Principal
NMIT

External Viva-Voce

Name of Examiners

Signature with Date

1.

2.

Acknowledgement

The successful execution of our project gives us an opportunity to convey our gratitude to each one who have been instrumental in paving the path to our continuation of this project.

We would like to thank and seek the blessings from **Dr. N R. Shetty**, Advisor, **Nitte Meenakshi Institute of Technology**, for his thrust on project-based learning and constructivist principles in our institution.

We would like to express our gratitude to the **Nitte Meenakshi Institute of Technology** and our beloved Principal **Dr. H C. Nagaraj** for providing us with the support, facilities and motivation to carry out our project.

We express our gratitude to **Dr. P.N. Tengli**, Professor and Head, Department of Aerospace and Defence R&D Centre, for providing us with all the required components and laboratory for manufacturing and testing of the UAV system.

We express our gratitude to **KSCST**, for providing us with funding of **INR 5000/-** for the project.

We express our deep sense of gratitude to **Dr. Parameshachari B D**, HOD, Department of Electronics and Communication Engineering, for his kind co-operation, valuable guidance and creating the best learning environment for us.

We wholeheartedly thank our guide **Dr. Murthy M**, Assistant Professor, Department of Electronics and Communication Engineering, for his/her support and guidance anytime we required.

We also thank and share this moment of happiness with our parents who rendered us enormous support during the whole tenure of our studies at Nitte Meenakshi Institute of Technology, Bengaluru.

Finally, we would like to thank all other unnamed who helped us in various ways to gain knowledge and have a good training.

Chaya R	(INT21EC037)
Mohit Mohan	(INT21EC085)
Venu V Muthyala	(INT21EC169)

Place: Bengaluru

Date: 21-06-2025

Abstract

Unmanned Aerial Vehicles (UAVs) or drones, have automated and taken over tasks that are dangerous, tedious, and perform tasks that difficulty or inaccessible to humans. This study presents usage of a H-Frame drone integrated with a sprayer system, to perform the task of maintenance of high-rise buildings and solar panels. The primary motivation driving this research is to mitigate the risks associated with human labour in cleaning of high-rise building facades and automating the tedious task of maintaining the solar panels in huge solar farms, in order to improve efficiency and safety of these operations. The H-frame design was chosen due its inherent advantages in operations in adverse weather, and superior cargo capacity and its excellent stability with heavy and large volume payloads with uneven weight distribution.

The core of the UAV system is the Pixhawk 2.4.8 flight controller, which provides excellent stability and precise control through a pilot-in-the-loop control law. In this law the pilot is mainly in control of the drone but the system provides active assistance to the pilot with features like loiter mode, altitude hold and failsafe functions like automatic return-to-home and a safe auto-landing in low battery conditions or a signal loss contingency which contribute to the increased safety and reliability of the system. The propulsion architecture employs a coaxial quad rotor configuration which allows for a higher thrust-to-weight ratio while keeping the overall size of the UAV compact.

The onboard sprayer system has a 1 litre storage tank which utilizes a diaphragm pump with a discharge rate capable of 5L/min combined with two sweeping servos to achieve wide-area coverage during cleaning operations. The system demonstrated a flight time of six minutes when carrying a payload of 3.5kgs, with the total system weight of 6 kg. Testing of the system included an autonomous hover test and manual flight operation to clean a window. Both tests showed the robust stability of the platform although the cleaning effectiveness was moderate, reflecting the prototype nature of the sprayer system, the primary objective of demonstrating the technology feasibility of an aerial maintenance vehicle was achieved successfully.

Overall, this work provided a practical foundation for future development of autonomous aerial maintenance systems, aiming to reduce human labour risks, improve safety, and deliver scalable systems with swarm drones for industrial solutions.

Table of Contents

Acknowledgement	1
Abstract	2
Table of Contents	3
Table of Tables	5
Table of Figures	6
Chapter 1: Introduction	7
1.1 Overview	7
1.2 Motivation	7
1.3 What are Drones?	8
1.4 Types of Drones	8
1.5 Applications of Drones	9
1.5.1 Industrial and Manufacturing Applications	9
1.5.2 Solar Panel Cleaning and Maintenance	10
1.5.3 Additional Applications of Drones	11
1.6 Control Algorithms and Stability	11
1.7 Public Perception and Societal Impact	12
Chapter 2: Literature Survey	14
2.1 Background Work	14
2.2 Open Issues and Challenges	26
2.3 Problem Definition	27
2.4 Objectives	28
2.5 Scope of the Work	29
2.6 Milestones	30
Chapter 3: Design Approach and Methodology	31
3.1 Control Architecture	31
3.2 Superiority of H-Frame over X-Frames	32
3.3 Superiority of Coaxial Quad over Octocopter	33
3.4 Thrust Calculation	34
3.5 Overall Design Configuration	36
Chapter 4: Implementation Details	38
4.1 Control Mechanism of Drones	38
4.2 PID and EKF algorithms	39
4.3 Motor Mixing for Coaxial Quad	41

4.4.	Hardware and software description	42
4.4.1.	Hardware Components	43
4.4.2.	Software Tools	43
4.5.	Key Specifications	44
4.6.	Sprayer System	45
4.7.	Power and Electronic Speed Control:	46
4.8.	Communication and Control:	48
Chapter 5:	Results and Analysis	50
5.1.	Autonomous Flight	50
5.2.	Sprayer System Tests	51
5.3.	Manual Flight	52
5.4.	Final Inference	54
5.5.	Flight Logs	55
Chapter 6:	Conclusion and Future Scope	60
6.1.	Future Scope	60
	Bibliography	62
	Appendix – A	66
	Appendix – B	67
	Publication Details	68

Table of Tables

Table 1: Table showing the specifications of the motor used to power the drone's propulsion system	35
Table 2: Table summarizing the final thrust calculations values obtained from the design iterations	35
Table 3: Table presenting the motor labels and its respective directions for an X8 configuration drone.....	41
Table 4: Table presenting the motor mixing matrix for an X8 configuration drone	42
Table 5: Table stating the major hardware components used the prototype UAV system.....	43
Table 6: Table summarising the key specifications of the UAV system.....	45
Table 7: Table summarizing the UAVs power system parameters	48
Table 8: Table summarizing the communication system of the drone.....	49
Table 9: Table showing the results of the three autonomous flights	51
Table 10: Table showing the manual flight test results by Pilot 1.....	53
Table 11: Table showing manual flight test results by Pilot 2	54
Table 12: Table showing the final inference of the result analysis	55
Table 13: Table showing Pixhawk 2.4.8 parameter tree values	67

Table of Figures

Fig 1: Image of the top view of the prototype drone with a GPS lock in a ready to take-off condition.	7
Fig 2: Image of H-Frame drone with the sprayer system performing an autonomous hover mission at an altitude of 3m AGL to test stability of the system.	10
Fig 3: Block diagram showing the control architecture and power flow of the UAV and the sprayer system.	31
Fig 4: Image showing the isometric view of the CAD model showing the different parts of the drone	36
Fig 5: Image showing the left side view of the CAD model showing the different parts of the drone	37
Fig 6: Image showing the degrees of freedom of a multicopter with an inertial frame of reference	38
Fig 7: Block diagram of the control flow of the signals from the outer loop to the inner loop and finally to the motor ESCs	39
Fig 8: Motor configuration diagram showing the X8 motor labelling	41
Fig 9: Image representing the NED directions in multicopter.	42
Fig 10: Screenshot of the HUD and map display of the mission planner software	44
Fig 11: Block diagram showing the control flow of the sprayer system	45
Fig 12: Image showing the working of a classical diaphragm pump	46
Fig 13: Block diagram showing the flow of electrical power in the UAV system.	46
Fig 14: Block diagram showing the working of the communication system of the UAV	48
Fig 15: Image showing the initial testing of the sprayer system on the ground	52
Fig 16: Image showing the drone performing a manual cleaning operation on a window.	53
Fig 17: Graph showing the UAV's flight path acquired from the GPS data where x-axis is the latitude and y-axis is the longitude with a google earth 2D image overlayed in the background for easier referencing	55
Fig 18: Graph of GPS altitude data in meters (x-axis) plotted over time in seconds (y-axis) showing the change in altitude during the flight.	56
Fig 19: Graph showing the change in measured battery voltage in volts (x-axis) over time in seconds (y-axis) during the flight indicating consistent drop of voltage over time	56
Fig 20: Graph of GPS latitude data in degrees (x-axis) plotted over time in seconds (y-axis) showing the change in latitude during the flight.	57
Fig 21: Graph of GPS longitude data in degrees (x-axis) plotted over time in seconds (y-axis) showing the change in longitude during the flight.	57
Fig 22: A graph showing the pitch angle in degrees (x-axis) against time in seconds (y-axis) indicating the attitude of drone in the pitch axis for the entire flight	58
Fig 23: A graph showing the roll angles in degrees (x-axis) against time in seconds (y-axis) indicating the roll attitude of the drone for the duration of the flight.	58
Fig 24: Graph showing the yaw rotations performed in degrees (x-axis) over time in seconds (y-axis) during the test flight of the drone	59
Fig 25: Graph showing the indicated air speed of the drone in meters per second (x-axis) to the event time in seconds (y-axis) during the test flight of the drone	59

Chapter 1: Introduction

1.1 Overview

Drones, also known as Unmanned Aerial Vehicles (UAVs), are aircraft that operate without a human pilot on board. They are controlled remotely or autonomously through pre-programmed flight paths and onboard sensors. Originally developed for military use, drones are now widely used in various civilian applications such as aerial photography, agriculture, surveillance, delivery services, disaster management, search-and-rescue operations, construction, inspection. This project focuses on the development of an H-frame drone equipped with a sprayer system, specifically designed for high-rise building maintenance and solar panel cleaning. The drone incorporates onboard sprayer system with 1 Litre tank of water, and a servo mechanism to perform a sweeping motion of the sprayer improving the area coverage. The H-frame design allows more payload capacity [1] in both volume as well as mass, while maintaining stability in windy conditions. This innovation aims to enhance safety, reduce labour costs, and improve the efficiency of tasks that are traditionally hazardous and labour-intensive [2], [3]

Furthermore, the H-frame design ensures structural stability, making it suitable for operations at great heights and in adverse weather conditions. The potential for swarm deployment of such drones, as discussed by Suarez et al. [3], further amplifies their utility in large-scale maintenance projects.



Fig 1: Image of the top view of the prototype drone with a GPS lock in a ready to take-off condition.

1.2 Motivation

Maintaining and cleaning high-rise buildings is among the most dangerous jobs due to extreme heights, unexpected gusts, and potential falls [4], even with safety harnesses. Workers also face harsh weather conditions like intense heat, cold, or rain, leading to risks such as frostbite or heatstroke.

Accessibility is another challenge, as architectural elements like ledges and corners are often difficult to reach. Solar panel maintenance presents similar difficulties. If not cleaned regularly, panel efficiency can drop by 20–30% [5]. Cleaning on rooftops increases fall risks, and the fragile nature of solar panels makes them prone to damage.

Additionally, elevated temperatures during cleaning can harm glass, necessitating careful water use. Address these safety and logistical challenges, we propose developing a drone with a sprayer system to oversee these tasks, reducing labour costs, increasing safety, and paving the way for future automation.

This innovative solution could not only enhance operational efficiency but also promote the widespread adoption of drones in building maintenance and renewable energy sectors.

1.3 What are Drones?

Drones, or Unmanned Aerial Vehicles (UAVs), have revolutionized the way tasks are performed across industries by offering a cost-effective, efficient, and flexible aerial platform. In agriculture, one of the most impactful applications of drones is in the form of sprayer drones. These specialized UAVs are equipped with tanks and nozzles to spray fertilizers, pesticides, and other agrochemicals with high precision. Sprayer drones help reduce human exposure to harmful chemicals, minimize wastage, and increase coverage speed making them an essential tool for modern, smart farming practices.

Sprayer drones are increasingly being used in cleaning applications, especially for tasks that involve hard-to-reach or hazardous areas such as tall buildings, solar panels, and glass facades. Equipped with water tanks and high-pressure nozzles, these drones can effectively spray cleaning solutions or water to remove dust, dirt, and other debris. In solar panel maintenance, sprayer drones offer a safe and efficient alternative to manual cleaning, helping maintain optimal energy efficiency without risking worker safety. Their ability to cover large surfaces quickly and uniformly makes them a valuable tool for commercial cleaning operations and facility management.

1.4 Types of Drones

Drones come in various types depending on their design, purpose, and mode of operation. Broadly, drones can be classified into four main categories: multi-rotor, fixed-wing, single-rotor, and hybrid VTOL (Vertical Take-Off and Landing). Multi-rotor drones, such as quadcopters and hexacopters, are the most common and are favoured for their stability and ease of control, making them ideal for photography, surveillance, and recreational use.

Drone frames and configurations vary to suit specific tasks and flight characteristics. Common frame types include X-frame, H-frame, and + (plus) configurations, primarily seen in quadcopters. X-frames provide balanced agility and are ideal for racing or freestyle drones, while H-frames offer better payload distribution and stability, often used in industrial or cinematic applications. Multi-rotor configurations range from tricopters (3 rotors), quadcopters (4 rotors), hexacopters (6 rotors), to octocopters (8 rotors). Increasing the number of rotors improves lift capacity, redundancy, and stability but also increases power consumption and complexity.

Motor arrangements also differ based on design requirements. The most common is the standard single-motor per arm configuration, where each rotor is driven by a single motor. In coaxial configurations, two motors are mounted on the same axis but spin in opposite directions, allowing for greater thrust in a compact space and improved redundancy. This is commonly used in heavy-lift or VTOL systems. Some drones also use contra-rotating propellers to cancel torque effects and enhance stability. Understanding these technical configurations is crucial for optimizing performance based on the drone's intended application.

1.5 Applications of Drones

Drones have become a transformative technology across numerous sectors, offering innovative solutions to tasks that once required significant time, labour, or posed safety risks. Their ability to capture aerial data, access remote or hazardous areas, and perform tasks autonomously or semi-autonomously has made them indispensable in fields such as agriculture, surveillance, logistics, environmental monitoring, and emergency services.

Whether it's monitoring crop health with multispectral imaging, delivering medical supplies to remote locations, or assisting in search and rescue operations, drones provide speed, accuracy, and cost-efficiency. As their technology continues to evolve, the scope and impact of drone applications are expected to grow even further, addressing new challenges with smarter, more capable aerial systems.

1.5.1. Industrial and Manufacturing Applications

In industrial and manufacturing settings, drones are increasingly being utilized for tasks such as inspection, inventory management, and monitoring of large facilities. Their ability to quickly access elevated or confined spaces allows them to perform inspections of equipment like pipelines, storage tanks, and structural components without the need for scaffolding or human entry into hazardous areas. This not only enhances safety but also reduces downtime and operational costs.

For example, drones equipped with high-resolution cameras or thermal sensors can detect leaks, corrosion, or overheating in machinery and infrastructure, enabling predictive maintenance. In warehouses, drones can automate inventory checks by scanning barcodes or RFID tags on shelves, improving accuracy and reducing manual labour. Their capability to rapidly navigate complex environments and provide real-time data makes drones a valuable asset in modern industrial operations.

The H-frame drone developed in this project could also be adapted for industrial applications. The drone's stability in adverse conditions makes it suitable for operations in industrial environments, where factors such as heat, dust, or vibrations can pose significant challenges.

1.5.2. Solar Panel Cleaning and Maintenance

One of the key applications of the H-frame drone developed in this project is solar panel cleaning and maintenance. Solar panels are often installed in remote or difficult-to-access locations, such as rooftops or deserts, making their maintenance a challenging and labour-intensive task. Drones, equipped with cleaning tools and sensors, can perform these tasks more efficiently and safely.



Fig 2: Image of H-Frame drone with the sprayer system performing an autonomous hover mission at an altitude of 3m AGL to test stability of the system.

Alkaddour et al. [10] proposed a novel design for a lightweight aerial manipulator specifically for solar panel cleaning, demonstrating the feasibility of such systems in real-world scenarios. The drone developed in this project builds on this concept, incorporating an H-frame design to ensure stability and endurance. Its robotic arm enables precise cleaning tasks, such as removing dust or debris from solar panels, improving their efficiency and longevity.

The use of drones for solar panel cleaning not only reduces labour costs but also improves the efficiency of solar installations, contributing to the global transition to

renewable energy. Additionally, the potential for swarm deployment, as discussed by Suarez et al. [3], further enhances the utility of drones in large-scale solar farms.

1.5.3. Additional Applications of Drones

In the field of infrastructure, these systems are used for inspecting and repairing buildings, bridges, and wind turbines. For example, Ollero et al. [1] discussed the use of drones for inspecting wind turbine blades, a task that is both hazardous and labour-intensive when performed by humans. The ability of UAVs to access difficult-to-reach areas and perform precise inspections makes them invaluable in this context.

In agriculture, UAVs are employed for precision tasks such as fruit picking, crop monitoring, and pesticide application. Balayan et al. [1] explored the use of quadcopters with lightweight robotic arms for precision agriculture, demonstrating their potential to improve efficiency and reduce labour costs. Similarly, Suarez et al. [3] highlighted the use of drones for environmental monitoring, such as collecting samples from trees or monitoring wildlife in remote areas.

Another promising application is in disaster response, where drones can be deployed for search-and-rescue missions in hazardous or inaccessible areas. For instance, Lee et al. [7] demonstrated the use of drones for pushing movable structures in disaster scenarios, showcasing their potential for real-world applications. The ability of these systems to operate in three-dimensional space and interact with their environment makes them uniquely suited for such tasks.

The H-frame drone developed in this project is particularly well-suited for high-rise building maintenance and solar panel cleaning. These tasks are labour-intensive and present significant safety risks, particularly in extreme weather conditions. Additionally, the potential for swarm deployment, as discussed by Suarez et al. [3], further enhances the utility of UAVs in large-scale projects.

1.6 Control Algorithms and Stability

One of the most critical challenges in the design and operation of drones is ensuring stability during spraying tasks, particularly in dynamic and unpredictable environments. Stability is essential for maintaining control over the drone and the sprayer system, especially when interacting with external objects or operating in windy conditions. Advanced control algorithms play a pivotal role in addressing these challenges.

For instance, Lee et al. [11] developed a disturbance observer (DOB)-based robust controller for drones, enabling them to push movable structures with precision. Their work demonstrated that robust control algorithms can effectively compensate for external

disturbances, such as wind gusts or unexpected payload shifts, ensuring stable operation. Similarly, Malczyk et al. [12] explored multi-directional interaction force control in drones, emphasizing the importance of adaptive control strategies for handling varying interaction forces during tasks like grasping or pushing. Their research highlighted the need for real-time feedback mechanisms to adjust control parameters dynamically, ensuring stability even under external disturbances.

The integration of such control algorithms is particularly relevant for the H-frame drone developed in this project. Given its application in high-rise building maintenance and solar panel cleaning, the drone must maintain stability in windy conditions and during precise manipulation tasks. However, advancements in control algorithms, as demonstrated by Lee et al. [11] and Malczyk et al. [12], provide a strong foundation for addressing these challenges.

Future research in this area could focus on the integration of machine learning and artificial intelligence to enhance the autonomy and adaptability of control systems. For example, reinforcement learning algorithms could be employed to optimize control parameters in real-time, enabling drones to operate more efficiently in complex environments.

1.7 Public Perception and Societal Impact

The adoption of drones in various industries is not only a technological challenge but also a societal one. Public perception plays a crucial role in determining the acceptance and success of these systems. Research by Li and Janabi-Sharifi [9] provides valuable insights into public opinion regarding UAV systems. Their study revealed that while there is general acceptance of these systems for societal benefits, concerns about safety, privacy, and potential misuse remain prevalent.

For instance, the use of UAVs for tasks such as infrastructure inspection and disaster response are widely viewed as beneficial due to their ability to reduce human risk and improve efficiency. However, the deployment of these systems in urban environments raises concerns about privacy and noise pollution. Addressing these concerns requires not only technological solutions, such as improved safety features and noise reduction mechanisms, but also transparent communication with the public about the benefits and limitations of drones.

The societal impact of drones extends beyond their immediate applications. For example, Alkaddour et al. [10] highlighted the potential of UAVs to revolutionize the solar energy industry by automating the cleaning and maintenance of solar panels. This not only

reduces labour costs but also improves the efficiency and longevity of solar installations, contributing to the global transition to renewable energy. Similarly, the use of UAVs in agriculture, as discussed by Balayan et al. [1], can enhance food production by enabling precision tasks such as crop monitoring and selective harvesting.

To ensure the successful integration of drones into society, it is essential to address public concerns through regulatory frameworks, public engagement, and continuous improvement of safety and privacy features. By doing so, UAVs can be positioned as a transformative technology that benefits both industry and society.

Chapter 2: Literature Survey

2.1. Background Work

Muhannad Alkaddour et. Al. [13] have developed a drone equipped with a COG compensation mechanism for cleaning solar panels, featuring a slider mechanism arm beneath the aerial platform. Their manipulator reduces COG shift during arm movement, enhancing stability by 34.5%. While the model includes tilt angle and slider position, the experimental validation is based on a fixed setup, which may not fully represent real-world conditions. The study overlooks factors that could affect cleaning efficiency, such as weather variations and panel configurations. Therefore, the proposes real-world testing to address deficiencies from static testing. Additionally, the H-frame design better handles COG shifts and wind resistance, improving stability margins.

Another COG compensation method was developed by Ibrahim Abuzayed et. Al. [10] for pick-and-place operations, utilizing a pantograph mechanism with a 3D-printed weight to actively balance the COG. Experiments conducted on a test bench demonstrated a maximum tilt of only 2.5 degrees with the counterweight, compared to 12 degrees without it, reflecting a 79% improvement. However, since this system was not tested on an aerial platform and involves more moving parts, it may not be as feasible as a slider mechanism, particularly for cleaning applications on drones.

Another capability of drones was demonstrated by Dongjae Lee et. Al. [14], who used a drone to push movable objects. They showed that unmanned drones can interact with structures weighing up to 42 kg. The drone was able to pitch up to 30 degrees to achieve efficient pushing. They proposed a novel algorithm to generate end-effector position references tailored for pushing tasks and demonstrated successful experiments with both a rolling cart and a hinged door, showcasing the feasibility and safety of the proposed method. However, the drone was entirely battery-powered, limiting its operational time. A foldable robotic arm for drones was developed by Wesley Thomas et. Al. [11], featuring a single actuator for both arm and case movements to minimize weight. The arm extends nearly five times its closed length, with a half-cylindrical case for compact storage. Motion analysis addressed kinematic singularity challenges by optimizing arm angles, but real-world testing may differ from the scaled 3D-printed prototype. Material choices like PLA/ABS offer lightweight benefits but may lack the strength needed for demanding tasks. The design focuses on UAV compatibility, yet incorporating springs for better functionality could add unwanted weight, compromising the lightweight goal.

The paper by Suthar and Jung [11] presents a foldable robot arm for drones (FRAD) using a twisted string actuator (TSA). The arm features a scissor mechanism designed for payload lifting to 0.3 kg without requiring drone landing. The TSA system exploits nonlinearity to optimize actuation, while a linkage design addresses mechanical singularity, improving foldability. Experiments confirmed the FRAD's capability for smooth folding and unfolding. However, joint clearance affected complete folding, reducing space-saving efficiency. Future work could integrate a gripper and compensate for hysteresis using nonlinear controllers to enhance overall functionality.

Flying Platforms (NTPFs), [15] highlighting their role in future wireless communication infrastructures, particularly in the context of Sixth Generation (6G) technologies. The study outlines the various types, components, and applications of NTPFs, noting their advantages in terms of endurance and cost-efficiency. However, it acknowledges the limitations of NTPFs, such as mobility constraints and tether length restrictions. The paper also emphasizes the need for a comprehensive analysis of NTPFs' wireless communication capabilities, including channel modelling and economic aspects. Nonetheless, the authors point out the lack of detailed technical discussions and practical case studies, suggesting that further research is necessary to explore the full potential and challenges of integrating NTPFs into non-terrestrial networks.

A novel single-wire earth-return (SWER) power transfer system for aerial platforms was introduced by Wang S and Ludois D [16]. This system leverages capacitance to achieve earth return without physical contact, utilizing a quarter-wavelength helical resonator to optimize voltage gain. The research derives a theoretical model based on transmission line theory and presents an equivalent circuit model combining the resonator and tether impedance, validated through laboratory prototypes. Experimental results demonstrated the system's effectiveness, achieving 500 W power throughput with efficiencies of 93% for a 70 m horizontal tether and 92% for a 30-50 m vertical tether. However, the implementation may face challenges due to its complexity, potential environmental impacts on performance, and limited scalability for larger platforms.

Xin Jin et. Al. [17] authors conducted a detailed analysis using electromagnetic surface wave theory and Maxwell's equations, simulating the propagation of electromagnetic field energy through a model built with HFSS. Their experiments demonstrated successful power transmission of up to 300 W over 100 m and 135 W over 200 m. While the study provides significant insights into SWPT's theoretical and practical aspects, it acknowledges challenges such as power loss at high voltages and the impact of

nearby metallic structures on transmission efficiency. Further research is needed to develop more robust models for real-world applications. Field tests analysed energy demand based on drone weight, measuring average and instantaneous currents. Results highlighted energy consumption differences, identifying possible causes for minor result discrepancies. However, testing conditions may not fully reflect real-world applications. Voltage drops and cable length affected efficiency, suggesting the need for improved power management strategies in diverse environments.

A comprehensive review of quadrotor UAVs was conducted by Moad Idrissi et al. [18], covering advancements in applications, design, and control algorithms over the past decade. The study categorized mechanical structures and explored VTOL configurations. It examined the dynamics and control strategies, highlighting the impact of disturbances on quadrotor performance. The review identified limitations in current control techniques, suggesting mechanical enhancements for improved stability. As a research gap, further study on control methods and analysis of H-frame drones will be explored to address these limitations and enhance UAV performance.

Anurag Balayan et al. [19] explored the optimal design of quadcopter chassis using generative design and lightweight materials for precision agriculture. The research focused on comparing H-frame and X-frame designs, revealing that H-frame configurations provide up to 30% more stability in hover and allow for an increased payload capacity of 25% compared to X-frame models. Advanced design methodologies were employed to optimize structural performance while minimizing weight. However, the results may not fully translate to practical agricultural settings due to unaccounted environmental variables during testing. Additionally, the reliance on specific lightweight materials could limit design versatility in varied operational conditions.

The structural design of quadcopter UAVs explored by Luttfi A. Al-Haddad et al. [1] using topology optimization and additive manufacturing techniques. The study emphasizes the importance of lightweight materials, achieving significant weight reduction of approximately 30% compared to traditional designs. The research highlights the advantages of H-frame designs over X-frame configurations, noting that the H-frame's stability in hover conditions is enhanced due to its wider stance and lower centre of gravity, which improves payload capacity by 25%. However, the paper does not extensively address the specific aerodynamic efficiencies between the two frame types. Limitations include a lack of real-world testing scenarios, which may affect the applicability of the design

parameters in various operating conditions. The complexity of additive manufacturing processes also presents potential challenges in scalability for commercial applications.

A design study for a dual-arm aerial manipulator was conducted by Alejandro Suarez et al. [7], focusing on Standard and Long Reach configurations. The Standard Configuration integrates arms at the base of the multirotor, while the Long Reach Configuration employs a pendulum mechanism for an operational range extension of 20 cm, enhancing safety in challenging environments. This manipulator aims to replicate human dexterity for tasks like sensor installation, achieving task completion times as low as 30 seconds. However, the complexity of the control algorithms for stability makes it less feasible for the proposed solution, posing challenges that could hinder practical cleaning applications where simplicity and reliability are crucial.

A hybrid motion-force controller for drones was developed by Grzegorz Malczyk et al. [8], enhancing drones' ability to perform push-and-slide tasks while resisting external disturbances such as wind. The research integrates an Extended Kalman Filter (EKF) for estimating disturbances, resulting in a disturbance rejection rate exceeding 90%. However, the advanced control algorithms introduce complexity that may not align with the simplicity required for H-frame robotic arm cleaners. This intricate system could hinder practical implementation, as cleaning tasks typically prioritize reliability and ease of use.

Walendziuk W et. Al. [12] analysed three power supply topologies for drones: two-stage systems with distributed supply and load balancing, and a simpler single-stage system with transformer isolation. While the two-stage systems offer better reliability, the single-stage is less efficient and fault-tolerant. The study identifies the increased weight of power components as a drawback, potentially limiting payload capacity. Despite valuable insights, the paper lacks concrete testing results and experimental validation, highlighting the need for further practical studies to verify these findings.

A systematic review of UAVs was provided Marques et al. [20], focusing on their applications, propulsion, energy transfer methods, sensors, and control techniques. The study identifies multirotor as the most used UAV type, particularly in load transport and long-endurance missions. It highlights high-voltage DC transfer as the preferred energy method, although many studies lack detailed descriptions of energy transfer solutions. The review also notes the prevalence of Proportional–Integral–Derivative (PID) control schemes across the literature. A key drawback is the absence of experimental validation in many studies, with theoretical models dominating the research. The authors recommend

further investigations into energy transfer methods and tailored control strategies to improve performance in specific applications.

Chang and Hung [21] present the design and implementation of a tether-powered hexacopter aimed at overcoming the endurance limitations of traditional battery-powered drones. The study outlines a power management system that enables continuous flight by drawing power from a ground station via a tether. The hexacopter was shown to achieve significantly longer flight times, making it suitable for long-endurance missions like surveillance and environmental monitoring. Key challenges highlighted include tether length constraints and power losses over long cables, which can limit the drone's range and efficiency. The authors provided performance data, with flight endurance exceeding 4 hours, but suggested further research into optimizing power delivery and minimizing weight to improve operational flexibility.

Phang et al. [6] present the design, dynamics modelling, and control of an H-shaped multi-rotor system optimized for indoor navigation. The study focuses on stability and manoeuvrability in confined spaces, leveraging an H-frame structure to enhance control. Experimental results showed that the proposed model achieved a position error of only 5 cm during navigation tasks. However, limitations in handling external disturbances were noted, especially under turbulent conditions. The authors suggest further research to refine control strategies and improve robustness and precision in various environments.

In order to improve maintenance efficiency in large-scale solar farms, Liao and Lu [22] suggest a UAV-based system for identifying solar module faults using integrated infrared (IR) and visible light imaging. The system uses MATLAB-based software in conjunction with UAV-mounted dual-lens cameras to detect flaws like contamination, hot spots, and cracks. The method uses a four-step process that includes grayscale conversion, Gaussian filtering, 3D temperature visualization, and statistical analysis using probability density and cumulative distribution functions. It has been validated through two-stage field experiments on ten real-world cases. The technique helps with timely maintenance decisions by precisely locating and quantifying flaws. However, issues like false positives caused by reflection in infrared images require cross-referencing with visible-light images. Even though the method is faster and more accurate than manual methods, it is still advised to refine it further in complex lighting and use AI for more sophisticated fault classification.

A UAV-based thermal imaging system was created by Pruthviraj et al. [23] to identify flaws in photovoltaic (PV) panels in expansive solar farms. The system surveyed 232,934 panels in a 55 MW South Indian solar field by combining RGB and infrared

cameras with geospatial mapping. With 97% accuracy, 2,481 defects were found. When compared to manual methods, the approach greatly decreased inspection time and operating costs. Among the difficulties were the need for exact flight planning, image overlap, and geotagging, as well as environmental sensitivities (dust, shading, and reflections) that affected thermal readings. In order to boost scalability and reliability, the authors suggest future advancements through AI-based defect classification (YOLOv5, for example) and improved robustness under complex conditions.

The design, production, and uses of fibre-reinforced polymer (FRP) composites are reviewed by Rajak et al. [24], who highlight the lightweight, high-strength potential of these materials for use in the construction, automotive, marine, and aerospace industries. They examine manufacturing techniques ranging from hand lay-up to sophisticated robotic winding, classify natural and synthetic fibres, and evaluate mechanical and thermal characteristics. Fiber hybridization and surface treatments give FRPs superior performance, corrosion resistance, and high strength-to-weight ratios. Defects like voids and delamination present difficulties, and synthetic fibres raise environmental issues. In order to increase sustainability and material efficiency, the authors support bio-based, recyclable composites and suggest further study into eco-friendly formulations, automated manufacturing, and enhanced recycling.

Shaw and Vimalkumar [25] present the design and development of an octocopter drone intended for agricultural applications, specifically for the spraying of pesticides, fertilizers, and disinfectants. The system uses a 22,000 mAh Li-Po battery to power a 12-volt pump, a 6-liter tank, a quad-nozzle sprayer, and an FPV camera. It can fly for 10.4 minutes, carry a 6.75 kg payload, and empty the tank in a single sortie. Public sanitation is one of the versatile applications supported by the modular design. Limitations include difficulties balancing payload for stability and a brief flight duration brought on by high power consumption. To increase productivity and expand operational capability, the authors suggest future improvements like image-based precision spraying, autonomous GPS control, and better battery management.

In their review of automated solar panel cleaning robots, Sarode et al. [26] address efficiency losses caused by dust and contaminants. They group solutions according to cleaning techniques (dry brushing, air, mist, vacuum) and drive mechanisms (wheel, tank tread, and holonomic). In water-scarce areas, dry-cleaning robots with tank treads and airflow are preferred due to their low water consumption and affordability. Technologies that provide web-based controls and autonomous navigation include Ecoppia T4 (Israel),

Shreem (India), and Resola (Japan). High prices, limited ability to adjust to slopes, complicated maintenance, and uneven cleaning on irregular surfaces are some of the difficulties. Future studies should incorporate IoT-based controls for flexibility and monitoring, improve cleaning on a variety of panels, decrease weight, and improve navigation.

Symmetrical diaphragm pumps are reviewed by Zhao et al. [27] for the transportation of volatile, viscous, and corrosive media in sectors such as wastewater treatment and petrochemicals. By focusing on advancements in cavitation resistance, wear reduction, and noise suppression, they examine the principles, structures, and types of pumps (mechanical, hydraulic, and pneumatic). Symmetrical designs increase longevity, decrease vibration, and improve stability. Efficiency and dependability are increased by advancements in fluid-structure models, diaphragm materials, and check valves. Noise, cavitation, and wear from solids are obstacles. For increased sustainability and durability, future studies should concentrate on entropy-based analysis, environmentally friendly materials, improved diagnostics, and advanced manufacturing.

In order to increase the uniformity of pesticide application, Ni et al. [28] developed a variable spray system for plant protection UAVs. The system incorporates multi-sensor data to dynamically modify UAV offset and nozzle output using CFD simulations and a back-propagation neural network (BPNN). Spray coverage errors in field trials were within 30%, while CFD predictions showed an error of less than 10%. The system decreased waste and improved accuracy. Environmental variability, boundary sensitivity, and computational load are obstacles. For increased robustness, future research should enhance real-time control, neural networks, and datasets.

Jaswal and Sinha [29] present a review on chemical self-cleaning methods for solar panels, with a focus on superhydrophobic nanocoating's designed to mitigate energy losses caused by dust accumulation on photovoltaic (PV) surfaces. They draw attention to coatings made of nanomaterials, particularly zinc oxide (ZnO) films, which repel dust and water by using the lotus effect. Superhydrophobic coatings increase transmittance and thermal stability while reducing daily power losses from 3.3% to 2.5%. The scalability of various fabrication techniques, such as spin, spray, dip coating, and chemical vapor deposition, varies. High production costs, reliance on rainfall in arid regions, and limited durability under abrasion are some of the difficulties. For wider use in solar farms, future studies should improve mechanical strength, coating adhesion, contact angles greater than 150° , and the development of affordable, scalable manufacturing.

Aljaghoub et al. [30] use a multi-criteria decision-making (MCDM) approach to evaluate photovoltaic (PV) panel cleaning techniques in light of the Sustainable Development Goals of the UN. Using the TOPSIS method, they assess four cleaning techniques—automated, manual, electrostatic, and natural—across 18 environmental, economic, and social criteria. Due to its financial advantages, manual cleaning came in first, whereas electrostatic cleaning works best in places with limited water supplies. The study highlights the need for additional research to enhance cleaning technologies' scalability, affordability, and durability as well as their integration with IoT systems for optimal deployment.

A drone-based system for aerial evaluation of solar panels is presented by Mekid and Faramarzi [31], who combine thermal and visible light imaging sensors on an autonomous UAV for fault detection. In addition to providing greater spatial coverage and real-time georeferenced imaging for improved defect localization, the system increases efficiency by cutting down on inspection time and labour. It successfully identifies issues that impair performance in massive solar farms, but it has drawbacks like low sensor resolution, environmental sensitivity, and the requirement for trained operators. For increased operational reliability and scalability, the authors advise future research to improve UAV flight stability, integrate automated image processing, and increase sensor accuracy.

An automated solar panel cleaning system is presented by Patil et al. [32] with the goal of minimizing energy losses due to dust accumulation. The system consists of an Arduino and infrared sensor-controlled rotating brush made of microfiber cloth that is mounted on a self-sufficient mobile frame. Particularly in places with limited water supplies, it efficiently eliminates dust, increasing power output and lowering maintenance costs. However, the system's dependence on single-axis movement, which limits flexibility, and its bulkiness, which limits portability, are drawbacks. To increase efficiency and scalability, the authors suggest future enhancements like foldable frames, dual-axis movement, Internet of Things-based monitoring, and features like integrated cameras and de-ionized water cleaning.

An integrated computational materials engineering (ICME) method is presented by Quigley et al. [33] for the analysis of carbon fibre rods for sporting goods, specifically fishing rods. To describe the mechanical characteristics of carbon fibre prepreg layups, the methodology combines experimental three-point bending tests with FEM simulations. The ICME approach is validated by key findings that demonstrate strong agreement between

simulated and experimental results for flexural stiffness and Young's modulus. Modal analysis, which is essential for fly fishing, is also included in the study to evaluate vibrational behaviour. Predictive modelling is impacted by manufacturing complexities such as uneven fibre alignment. In order to improve rod design and production, future research should concentrate on honing material property measurements, increasing simulation accuracy, and incorporating advanced material characterization.

A cost analysis of institutional green cleaning programs is presented by Espinoza et al. [34], who assess the viability of implementing environmentally friendly products in large facilities. According to the study, which contrasts 373 conventional and green-certified cleaning products, floor strippers can save a lot of money by using green products, particularly concentrates, which are frequently more affordable or competitively priced. Automatic dilution systems and microfiber mops also lower expenses while enhancing security and lowering the number of accidents. The need for specialized training, the higher initial costs of microfiber equipment, and possible performance trade-offs with safer alternatives are obstacles, though. In order to encourage a wider adoption of green cleaning practices, the authors suggest more research on the long-term savings from decreased absenteeism, lower healthcare costs, and environmental impact.

To learn more about how fabric care products and washing conditions affect microplastic pollution, Lant et al. [35] look into the release of microfibers from consumer laundry. They tested 79 wash loads under both North American and European conditions and found that while larger wash loads reduced shedding, colder, faster wash cycles decreased microfiber release by 30% and whiteness loss by 42%. High-Efficiency machines decreased shedding by up to 69.7%, while fabric softeners and detergent pods had no discernible effect. The prevalence of natural fibres in released microfibers, which are still environmentally significant, and variations in fabric type and washing machine design are among the difficulties. To lessen microfiber pollution, the authors advise more study into cold-water cleaning methods, testing procedures, and textile design.

A drone-based aerodynamic cleaning system for dust removal from photovoltaic (PV) panels in desert environments is presented by Mohandes et al. [36]. The system removes dust without the need for water or physical contact by using downward thrust from a multirotor drone. Important results indicate that, with heavy soiling, horizontal flight paths improved PV output by up to 69.4% and had the highest dust removal efficiency. Because they covered more ground, horizontal paths performed better than vertical and diagonal ones. Benefits include lower labour risks, water conservation, and maintenance

cost savings. Among the difficulties are the drone's 16-minute endurance limit, high startup costs, and diminished performance in extremely dusty or intricately designed environments. Optimized flight algorithms, increased battery capacity, and autonomous navigation should be the main areas of future research.

A foldable robot arm integrated into a drone (FRAD) for cleaning solar panels is presented by Choi and Jung [37]. It is intended for use in remote or difficult-to-reach areas. The FRAD's lightweight, s-shaped foldable structure maximizes stiffness while reducing aerodynamic drag. Important results demonstrate that the FRAD efficiently controls contact force and optimizes cleaning patterns based on contaminant distribution using hybrid force control and clustering algorithms (SOM, K-means), improving efficiency and battery conservation. The system's viability in controlled settings is confirmed by experimental findings. Nevertheless, difficulties include limited outdoor testing, decreased flight time because of the additional payload, and possible drone instability. Future advancements in manipulator design, force control algorithms, and practical field testing for scalability are all suggested by the authors.

In order to clean surfaces in hazardous and difficult-to-reach areas, Kim et al. [38] present a bio-inspired cleaning module for a wall-climbing drone. A peristaltic water flow control mechanism built into the CAROS-Q drone uses a single servo actuator to supply water to rotating brushes, lowering payload weight and guaranteeing uniform wetting. According to experimental results, water-soluble ink and dirt can be effectively removed with little water. A small water reservoir, restrictions on payload capacity, and restrictions on flat surfaces are among the difficulties. To increase operational capabilities, the authors suggest further study on modifying the system for sloping surfaces, enhancing water delivery effectiveness, and optimizing brush materials.

For automated solar panel cleaning, Nagaraj and Dey [39] suggest a hybrid drone system that combines a multirotor drone with a water spray and soft brush system. To increase operational uptime, the drone has a hybrid power system that allows for in-flight battery charging through a tethered power line. According to test results, compared to conventional methods, cleaning efficiency is increased and water usage is decreased. The intricacy of tethered flight and flight instability in wind, however, present difficulties that may restrict field deployment and scalability. For wider applicability, the authors recommend more research to improve real-time environmental adaptation and autonomous navigation.

Rahman et al. [40] introduce a radio frequency (RF) signal-controlled glass and wall cleaning drone designed to reduce human risk in high-rise maintenance tasks. Using a remote transmitter, the drone incorporates a cleaning module that includes a fibre-cloth roller and fluid dispenser. Time-controlled cleaning, onboard video streaming, and multiple flight modes are important features. The prototype improved safety and efficiently used less water. The quadcopter's limited payload capacity and flight stability present difficulties, though. In order to increase endurance and sustainability, the authors recommend future advancements like employing more durable hexacopter or octocopter platforms, incorporating autonomous navigation, and investigating solar-powered operation.

Mishra et al. [41] introduce a drone-based solar panel cleaning system that eliminates dust and pollutants to increase photovoltaic efficiency. The monocopter drone is equipped with AI-based image recognition models (CNN, YOLOv5) to detect soiled panels and uses downward thrust or brushes to remove dirt. For autonomous navigation, the system is verified in simulation environments such as Gazebo and MATLAB/Simulink. Although a 35% increase in efficiency and a 60% decrease in maintenance effort are promised, difficulties include expensive initial costs, short battery life, and the intricacy of integrating sensors and computing units. To improve scalability and practical performance, the authors advise refining sensor fusion and battery management.

In order to solve operational, safety, and financial issues, Al Hulaibi et al. [5] present SkyBot, an autonomous drone system for cleaning skyscraper windows. SkyBot has two fluid tanks, an air blower, a high-pressure washer, and a real-time video camera. It is powered by a DJI S1000 octocopter. Because of its cable-free design, cleaning at high altitudes is possible with little risk to people. According to performance tests, it could clean 3 m² in 20 minutes, which would save 47% on operating costs when compared to traditional methods. However, scalability and continuous operation are hampered by its short flight duration (15–20 minutes) and high take-off power (4,136 W). For greater viability in the real world, the authors suggest improving flight autonomy and battery endurance.

A semi-automatic quadcopter that sprays pesticides is presented by Fisol et al. [42] in an effort to lessen manual labour and chemical exposure in agriculture. The system offers a low-cost, smartphone-operated solution for small-scale farming by integrating a NodeMCU-based remote-controlled sprayer, an F450 frame, and a CC3D flight controller. Important results demonstrate partial flight stability and successful remote operation, underscoring the viability of UAV-integrated spraying. Nevertheless, difficulties include

wind sensitivity, obsolete flight control software (OpenPilot), and flight instability brought on by an unbalanced payload. Performance was further hampered by the drone's small payload capacity. For improved stability, lift, and autonomous capabilities, the authors advise upgrading flight controllers and utilizing more stable platforms, such as hexacopters.

For small farms and places with inadequate GPS coverage, Baidya et al. [43] create an autonomous drone that sprays pesticides without the use of GPS. For intelligent mapping, path planning, and obstacle avoidance, the system combines a Raspberry Pi 4, an ArduCopter APM 2.5 flight controller, and depth-sensing cameras. It generates a 3D field map for optimal spray coverage using SLAM and an AI algorithm. Using a web application for mission planning and real-time monitoring, the drone modifies its speed, altitude, and flow rate according to the type of crop. The system has issues with sensor integration and battery limitations, but it also lessens labour and its impact on the environment. For increased robustness and scalability, the authors suggest integrating machine learning and AI-based navigation.

Using 5G connectivity and AI-driven thermal imaging, Zou and Rajveer [44] create a drone-based solar panel inspection system that can identify photovoltaic flaws instantly. The system uses a quadcopter, an NVIDIA Jetson Nano, and a FLIR Duo Pro R thermal camera to take and process thermal images with CNN-29 and YOLOv4 models. Defects like cell failures, hotspots, and delamination are categorized by a custom AI pipeline using real-time GPS data sent to a ground station. The system's defect recognition confidence was 89%. Autonomous flight, remote monitoring, and effective data collection are benefits; however, high-performance computing requirements and dataset labelling are drawbacks. Pix4D integration and improving AI model generalization are examples of upcoming enhancements.

An autonomous inspection system for assessing solar panels and wind turbines is presented by Nguyen et al. [45] using Tello drones and the YOLOv8 object detection algorithm. Real-time video streaming and object classification are made possible by the system's use of a swarm of two quadrotor drones connected by a router. The drones use a customized YOLOv8 model that was trained on a dataset with five classes to identify flaws like dust and cracks. Successful detection with an average precision of 84.3% is demonstrated by case studies. However, detection accuracy was limited by the low-resolution cameras of the Tello drone, especially for subtle defects. In order to enhance performance and provide an affordable option for autonomous infrastructure inspection, the authors advise utilizing higher-resolution imaging and growing the dataset.

A deep learning-based framework for identifying and categorizing solar panel flaws using drone-acquired RGB and thermal imagery is presented by Terzoglou et al. [46]. The system uses an EfficientNet classifier to categorize faults into four types, a UNet model for interior segmentation, and YOLOv5 for panel detection. Using random forest classification, a thermal statistics analysis module additionally finds flaws that are invisible to the naked eye. The method had an 87% segmentation success rate, 90% detection confidence, and 95% classification accuracy. The use of high-quality image preprocessing, properly annotated datasets, and the limitations of synthetic training data are among the difficulties. For large-scale, real-time inspections, the authors advise incorporating this system into a completely autonomous drone.

Iversen, Birkved, and Cawthorne [47] offer an assessment framework that uses Environmental Impact Potential Assessment (EIPA) and Value Sensitive Design (VSD) to improve drone sustainability. The study examines two cases, a powerline inspection multicopter and a medical drone for blood transport, with an emphasis on long-term design, environmental cost, and stakeholder impact. Drones can cut greenhouse gas emissions by up to $11\times$ when compared to cars or helicopters, according to life-cycle assessments; however, manufacturing, particularly of carbon fibre and electronics, still has a major negative impact on the environment. The authors propose environmentally friendly substitutes that can reduce emissions by up to 13 times, such as thermoplastic composites and design-for-reuse. Problems include defining system boundaries and having too much faith in self-governing drones. The study promotes the early incorporation of social, ethical, and environmental factors into drone design.

2.2. Open Issues and Challenges

The literature survey identifies several research gaps and challenges in the development of drones and drones that can be addressed by the proposed H-frame drone design. Key points from the survey highlight the following:

1. **Complex Control Mechanisms:** Existing designs, such as those by Alejandro Suarez et al. [7] and Grzegorz Malczyk et al. [8], suffer from complex control algorithms, while the H-frame aims to simplify these for user-friendly applications.
2. **Inadequate Real-World Testing:** Heavy reliance on controlled environments in studies like those by Muhannad Alkaddour et al. [13] and Ibrahim Abuzayed et al. [10] necessitates extensive field testing for the H-frame design.

3. **Operational Limitations:** The need for lightweight solutions is emphasized by Walendziuk et al. [12] and Chang and Hung [21], who note tether length and weight constraints. The H-frame will optimize power usage to enhance endurance and flexibility.
4. **Environmental Impact Considerations:** Alouini and Belmekki [15] highlight the need for better analysis of environmental influences, which the H-frame design will incorporate.
5. **Lack of Experimental Validation:** Studies such as those by Marques et al. [20] reveal a gap in practical testing of energy transfer methods, which the H-frame aims to address.
6. **Handling External Disturbances:** Phang et al. [6] discuss challenges in managing external disturbances, indicating the H-frame's need for advanced stabilization techniques to enhance robustness.

By addressing these gaps, the H-frame drone aims to provide a more practical, efficient, and robust solution for aerial cleaning tasks, enhancing its utility in real-world applications while overcoming the limitations identified in current research.

2.3. Problem Definition

The increasing adoption of solar panels and the proliferation of high-rise buildings have created a growing need for efficient and safe cleaning solutions. Solar panels require regular maintenance to ensure optimal energy efficiency, as dust, dirt, and debris can significantly reduce their performance. Similarly, high-rise buildings often accumulate dirt and pollutants on their exteriors, which can affect their aesthetics and structural integrity over time. Traditional cleaning methods, such as manual labour or ground-based equipment, are often time-consuming, costly, and pose significant safety risks to workers, especially at great heights.

Currently, there is a lack of automated, cost-effective, and scalable solutions for cleaning solar panels and high-rise building exteriors. While some robotic systems exist, they are often limited in their adaptability, mobility, and precision. Additionally, many solutions are designed for specific applications and cannot be easily adapted to different environments or surfaces. This gap in technology highlights the need for an innovative system that can efficiently and safely clean both solar panels and high-rise buildings.

The primary problem this research addresses is the design and development of an H-Frame drone capable of performing cleaning tasks on solar panels and high-rise buildings. This system must be:

- **Adaptable:** Able to operate on various surfaces and structures.
- **Efficient:** Capable of cleaning large areas in a short time.
- **Safe:** Minimizing risks to human operators and the environment.
- **Cost-effective:** Providing a viable alternative to traditional cleaning methods.

The research will focus on addressing the following questions:

- What are the key design requirements for a drone to effectively clean solar panels and high-rise buildings?
- How can the system ensure stability and precision during operation?
- What technologies (e.g., drones, robotic arms, sensors) can be integrated to achieve optimal performance?
- How can the system be made cost-effective and scalable for widespread adoption?

By addressing these challenges, this research aims to develop a novel H-Frame drone that not only improves the efficiency and safety of cleaning operations but also contributes to the sustainability and maintenance of solar energy systems and urban infrastructure.

2.4. Objectives

The primary objective of this project is to build a drone that is capable of cleaning high rise buildings and solar panels in order to replace risky manual labour and improve precision and operational efficiency. Let's discuss the objectives in detail in the below section.

- **Design and Development of H-Frame Drone:** As our project includes a criterion for the use of H-Frame drone for the task we need to first design and build one which is capable of lifting the sprayer system and perform the task as H-frame drones are not that popular and ready to assemble kits as not available as much the market as per the requirements.
- **Building and Integrating Sprayer System:** The next task will be to design a suitable sprayer system that will perform the task of effectively cleaning the solar panels as well as the building facades, which should also be light enough to be carried by the drone.
- **Implementation of Control Systems:** After completion of the build proper control mechanisms needs to be implemented and tested for stability proper functioning of

all the systems. The drone should be easily controllable as it's a manually operated and hence should have simpler systems making it easy for a human operator.

- **Optimize Weight and Endurance:** The weight and endurance of a multicopter are directly proportional and hence work must be done to optimize weight as much as possible to increase endurance and hence giving more operational time, as systems must be made electrically and aerodynamically efficient to increase its flight time.
- **Fail-safes and operational safety:** Drones can be extremely deadly when not used properly or certain critical systems fail, hence redundant fail-safe mechanisms must be setup such as battery and fencing to improve operational safety.
- **Validate systems performance:** Lastly, we must validate the operational performance of the drone on the field from performing the tasks, fail-safes, endurance, and performance in high wind conditions and study its limitations.

2.5. Scope of the Work

This scope of this project focuses on the multidisciplinary design, prototyping and testing of a drone that can perform cleaning tasks on building facades and solar panels. While this project has demonstrated the task successfully and shows potential in the technology the project has some limitations as well which will be discussed in the further section.

- **Structural Design and Fabrication:** Firstly, a stable and heavy lift platform capable of carrying the sprayer system will be developed, fabricated and tested. This will include the structural design as well the electronics like the flight controller, motors, communication systems and much more.
- **Sprayer system development:** Next, a suitable sprayer system will be designed and assembled and tested for operations with the aerial platform built with tools like pumps, servos, nozzles, tanks and other components.
- **Control system architecture:** Flight control algorithms and sprayer system control will be implemented and tested. It will be checked on criteria like stability, reliability, precision and effectiveness.
- **Testing and Validation:** Flight tests will be conducted and real-world missions will be performed to validate the performance of the system and look for if the developed system matches the required standards that is needed to perform the tasks and practical feasibility of such a system.
- **Limitations:** This system will be a complete manually operated system which can only operate for a very few minutes in real-world scenario not making it

commercially viable or operationally friendly product. The system will just be a technology demonstration and feasibility study of the effectiveness of such a system. It does not follow any regulatory certifications for commercial operations but it does comply with most of the safety requirements and can be made fully compliant with certain modifications.

2.6. Milestones

The project is divided into clearly defined milestones to ensure systematic progress from conceptualization to final delivery. Each milestone outlines key activities, expected outcomes, and an indicative timeline to monitor and guide the development process.

- **Month 1:** Literature survey and requirement analysis was carried out studying the existing drone-based cleaning technologies, identification of requirements, and problem definition.
- **Month 2:** Involved conceptual design finalization of H-frame structure, and the sprayer system.
- **Month 3:** Was spent in procurement of components such as structural materials, motors, electronic components, sensors, and sprayer system.
- **Month 4:** Fabrication of the H-frame drone chassis and assembly of propulsion system was done.
- **Month 5:** Development and attachment of the sprayer system with control interfaces for the servos and ground testing of the system.
- **Month 6:** Implementation of flight stabilization algorithms, and sprayer system control.
- **Month 7:** The built prototype was tested in laboratory, field trials, and performance analysis.
- **Month 8:** Documentation of the test results, analysis, and finalization of thesis report.

Chapter 3: Design Approach and Methodology

The development of the H-Frame drone for cleaning solar panels and high-rise buildings will follow a phased approach to ensure efficiency and reliability. The design will focus on creating a stable H-Frame drone using lightweight materials like carbon fibre, with high-performance motors and propellers for precise flight dynamics.

A sprayer system with two servos provides a sweeping motion will be developed to clean surfaces effectively while remaining lightweight and compatible with the drone. The system will undergo simulations and controlled testing to evaluate stability, cleaning efficiency, and durability.

Design refinements will optimize the drone's flight dynamics and the sprayer's functionality, ensuring seamless integration. Final field tests will validate its performance for real-world cleaning tasks, such as high-rise building facades and solar panels, providing a reliable solution for challenging environments.

3.1. Control Architecture

The architecture of the drone system ensures reliable power distribution, efficient communication, and precise control of all integrated components. The system is powered by a 6S 6800mAh LiPo battery, which supplies energy through a power module to manage stable voltage levels for different subsystems.

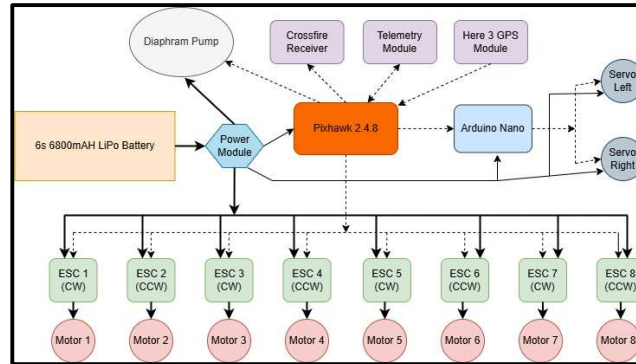


Fig 3: Block diagram showing the control architecture and power flow of the UAV and the sprayer system

At the core of the control system is the Pixhawk 2.4.8 flight controller, which processes pilot commands received via the Crossfire Receiver and relays necessary control signals to the ESCs (Electronic Speed Controllers) and servo motors. The Pixhawk is also interfaced with a telemetry module, enabling real-time data transmission for monitoring and adjustments.

The propulsion system consists of eight brushless motors controlled by corresponding ESCs, configured in alternating CW (Clockwise) and CCW (Counter-

clockwise) directions to ensure stable flight dynamics. The Cube Orange directs these ESCs to regulate the motor speeds accordingly.

Additionally, the drone incorporates an Arduino Nano, responsible for managing servo motors that assist in mechanical operations, likely related to the sprayer system. The diaphragm pump is integrated into the system, for spraying and cleaning functions, and is controlled through the Pixhawk.

This architecture ensures seamless integration of flight control, power management, and cleaning mechanisms, enabling stable operation and efficient execution of its intended tasks.

3.2. Superiority of H-Frame over X-Frames

Typically, X-Frames are more popular in drones compared to H-Frames or rectangular frames as they are much simpler in construction, more agile, and versatile than H-frames. They have their drawbacks which make it unsuitable for the tasks our platform is expected to perform.

Firstly H-Frame are more stable in hover than X-Frames. They sacrifice their agility for higher stability in hover, which is about 30% more stable than X-Frame [14], which is ideal for a platform that is supposed to stationary for longer periods of time and have multiple working attachments, for example maintenance of a solar panel or high-rise building. Its good stability also acts as an advantage for working in high crosswind conditions which is a challenge while working on high-rise buildings, which would be a bit of challenge for a X shaped drone for a comparable size.

Another characteristic of H drone is that it has a better handling with a moving CG, which is important because with movable attachments like sprayer systems and actuators the drone should be able to handle the shifts in CG very well as its working in proximity to obstacles which gives it less time and space to move around to adjust itself.

Most important of a H-Frame drone is its capability in carrying payloads. It can not only carry about 25% more [14] but also more volume and with multiple attaching methods. There is much more space, more attachment points for mounting attachments and flexibility in choosing the attachment points on the arms of the drone or main body of the drone.

Due to the unique spacing of H Drone propellers compared to an X-Frame each propeller gets cleaner air to generate thrust efficiently and this allows the mounting of more powerful motors and larger propellers increasing the weight carrying capacity of the frame.

Lastly, maintenance of a H-Frame with multiple attachments is easier as it has easier access to all the mounting points compared to a X-Frame whose mounting points are more compact and difficult to access.

3.3. Superiority of Coaxial Quad over Octocopter

Typically, octocopters are more commonly used in heavy-lift drone applications due to their redundancy and increased thrust capacity. However, coaxial quadcopters offer distinct advantages that make them more suitable for specific tasks, particularly where efficiency, compactness, and manoeuvrability are critical.

Firstly, a coaxial quad offers a more compact design compared to an octocopter, which has a larger frame due to the spread-out placement of its eight motors. This compact structure allows for easier deployment in constrained environments, making it more practical for operations in urban or confined spaces.

Another key advantage of a coaxial quad is higher thrust-to-weight efficiency. By stacking motors coaxially (one above the other), the drone achieves the same thrust output as an octocopter while reducing overall frame weight. This improves power efficiency, leading to longer flight times and reduced energy consumption compared to a traditional octocopter, which distributes its motors over a larger footprint and inherently has more structural weight.

The coaxial configuration also enhances aerodynamics by minimizing drag. With fewer extended arms than an octocopter, a coaxial quad reduces air resistance, making it more efficient in high-speed flight and operations in high-wind conditions. This is particularly useful in applications such as aerial inspections and high-rise maintenance, where stable positioning in challenging environments is essential.

One of the most important aspects of a coaxial quad is its superior payload capacity relative to frame size. While an octocopter has eight motors distributed across eight separate arms, a coaxial quad uses the same number of motors but in a more compact layout, allowing it to carry heavier payloads without increasing its overall frame size. Additionally, the coaxial design provides better load distribution, making it more stable when carrying external equipment such as robotic arms, sensors, or spraying systems.

Another crucial advantage of the coaxial configuration is its better handling of Centre of Gravity (CG) shifts. With payloads like sprayer systems or dynamic attachments, CG can change mid-flight. A coaxial quad, having a denser and more centralized weight

distribution, can adapt to these shifts more efficiently than an octocopter, which has its motors spread out, making CG changes more impactful on stability.

Lastly, maintenance and repair are more straightforward in a coaxial quad compared to an octocopter. With fewer arms and a more compact frame, accessing key components such as motors, ESCs, and wiring is significantly easier, reducing downtime and improving reliability in field operations. In contrast, an octocopter's spread-out design increases the complexity of maintenance, requiring more extensive structural disassembly.

In summary, while octocopters are widely used for their redundancy, the coaxial quad offers superior efficiency, compactness, higher payload capability relative to size, and improved handling in dynamic conditions. These advantages make it an ideal choice for applications where manoeuvrability, efficiency, and payload stability are crucial.

3.4. Thrust Calculation

Every flying craft is subject to four different forces namely, thrust, drag, lift, weight. In a multicopter the craft gets its lift from the propellers spinning and generating downward force by pushing the air equal to the weight of the craft. Hence, it is important to calculate the required thrust for a copter before deciding the configuration based on the assumed weight of the craft. It is an iterative process of the design where in for all the components weight is calculated then required thrust and then based on the suitable motors performance the thrust is recalculated and the new weight.

Based on the flight time of the initial configuration the battery or fuel weight is adjusted and thrust and weights are recalculated and finalized. Generally, the thrust to weight ratio for a multicopter is recommend to be about 1.5-2:1 so that the craft can take-off and hover at half the power and the motors are not running on full power.

For our design based on our calculations and components our weight of the drone will be about 7 kilograms when fully loaded and about 4 kilograms without the sprayer system. Considering this we will require a thrust of about 14 kilograms to have thrust to weight ratio of 2:1 which would be best for agility and better control. But since we did not have motors with such huge thrust available during the project our aim was to produce enough thrust to at least have thrust to weight ratio of 1.5:1 or higher.

Based on the requirement the required max thrust to be generated by the propulsion system should be,

$$\begin{aligned} \text{Required Thrust } (Tr) &= 1.5 \times \text{Weight } (W) \\ Tr &= 1.5 \times 7 = 10.5 \text{ kg} = 10500 \text{ g} \end{aligned}$$

Now we can consider the thrust produced by each motor and then we can calculate the total thrust we are getting out of the system. This information can be got from the motor data sheet or by manually testing it on a thrust test stand. So thrust produced by each motor according to the data sheet is,

Parameter	Value
Motor	FlyCat 5010
kV Rating	360 kV
Motor Type	Disc BLDC Motor
Propellor	14 x 5 inch
Motor Prop Mount Type	T-mount
Voltage	25.2 V
Thrust at 50%	545 g
Thrust at 75%	856 g
Thrust at 100%	1380 g
Current Idle	7.5 A
Current at 100%	25 A

Table 1: Table showing the specifications of the motor used to power the drone's propulsion system

Based on the data sheet the max thrust of the motor is 1380g and hence the total thrust developed by 8 motors will be,

$$\text{Thrust Generated (Tg)} = \text{Thrust per Motor} \times \text{No. of Motors}$$

$$Tg = 1380 \times 8 = 11040g = 11.04 \text{ kg}$$

$$Tg \approx 11 \text{ kgs}$$

Now we verify if the thrust to weight ratio is above 1.5:1 which means,

$$\text{Thrust to weight ratio} = \frac{Tg}{\text{Weight}} = \frac{11}{7} = 1.5 \approx 1.6:1$$

Parameter	Value
Total Weight	7 kgs
Dry Weight	4 kgs
Max Thrust per Motor	1.38 kgs
Max Thrust of the Drone	11 kgs
Thrust to Weight Ratio (With Payload)	1.6:1
Thrust to Weight Ratio (Dry Weight)	2.7:1

Table 2: Table summarizing the final thrust calculations values obtained from the design iterations

Hence, the propulsion system chosen will work for our application under fully loaded drone and can be considered for manufacturing of the drone. Here is a final table showing all the inferences of the thrust calculations.

3.5. Overall Design Configuration

After all the careful consideration of all the factors the final design configuration was decided and designed in Autodesk Fusion 360 software. The frame chosen was a H-Frame design with co-axial motor configuration. Such design was chosen because of the higher payload capacity requirement and also with the intention of making the drone as compact as possible.

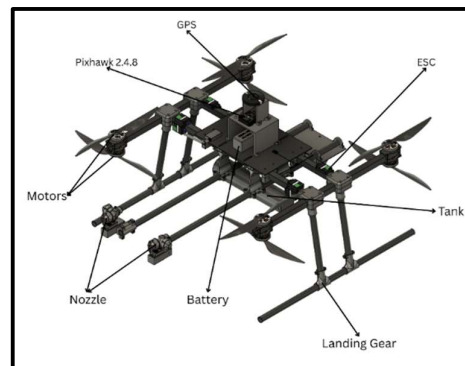


Fig 4: Image showing the isometric view of the CAD model showing the different parts of the drone

Here 3D Printed mounts were used to join the different carbon fibre rods. The prints were made of ABS plastic and PETG filament. This is because both these filaments are easy to print and have good strength compared to other filaments. It was decided to have all the main electronics mounted on the top of the central carbon fibre plate which is strong enough to hold the weight of the heavy battery. The carbon fibre allows for easy mounting of any components with simple 3D printed attachments.

The GPS is mounted at the highest level while the Pixhawk flight controller is mounted in the second level from the GPS and is placed over the battery. The receiver antenna and the telemetry module along with the safety switch is taped on to the carbon fibre plate as they do not require any kind of mount and carbon fibre plate offers a good space to mount the components.

The motors are mounted with 3D printed carbon fibre mounts which provide extremely good strength for their weight. Despite having ABS filament, we choose the more expensive carbon fibre mounts as its lighter and increases the factor of safety lot more than the ABS mounts and doesn't wear over time which is important for such a structurally

critically mount. The carbon fibre propellers required a spacer to be mounted on to the motor which was also 3D printed using the same carbon fibre filament.

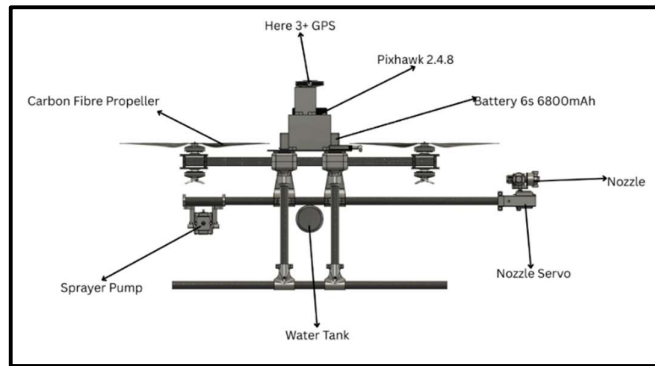


Fig 5: Image showing the left side view of the CAD model showing the different parts of the drone

The sprayer system is attached to a universal mount which can hold a 20mm carbon fibre tube. The pump is attached at the rear end and the nozzles in the front end of the system as the pump with its higher weight can counter the CG offset by the lighter by further away (longer lever arm) nozzle while staying closer to the drone. The tank was mounted in the centre of the drone it eliminates any CG offset to occur during the flight when the tank water quantity changes hence reducing its weight and therefore can affect the CG of the craft. The water tank also has 3 baffles creating 4 sections within the tank to prevent sloshing of water within the tank when flying hence balancing the dynamic CG of the drone.

Overall, this design was done considering all the factors based on the required flight time, lift capacity, available components, while trying to optimise cost as well as making a system that is as easy to assemble as possible to help in easy troubleshooting of the system as when required.

Chapter 4: Implementation Details

4.1. Control Mechanism of Drones

As mentioned earlier, the configuration of the drone we built is a coaxial quad which has one motor on top of the other and rotates in the opposite direction. For this type of design, there are specific control mechanisms that are universal to almost all multicopters. but differ in a few factors like motor mixing algorithms, and attitude control. Control mechanisms change based on the number of motors, placement of motors, and shape of the frame of the multicopter, and also direction of the nose (front) of the copter.

There are many very well developed firmwares available to control multicopters of almost all kinds of configurations. We choose to run the arducopter firmware is which is one of the most popular and best open-source firmware which is specifically developed for the Pixhawk flight controller we are using. We can program the flight controller using the software like mission planner or QGround Control. In our case we are using mission planner as its one of the easiest software to run and program a flight controller. We can also design and run our own custom LUA scripts on the copters using mission planner. Mission planner also has features like parameters tree and better HUD and gauges layout compared to QGround Control which is best for manual and semi autonomy operations like the ones are running.

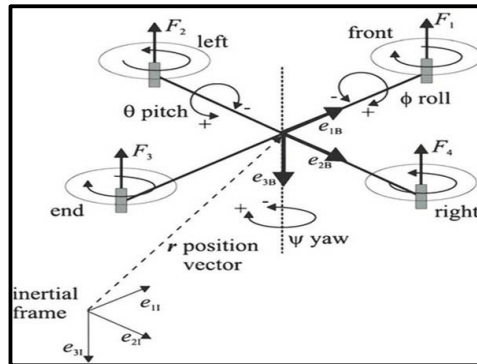


Fig 6: Image showing the degrees of freedom of a multicopter with an inertial frame of reference

Multicopters cannot fly without an active flight control. They are basically bricks constantly trying not to fall out of the sky, about 400Hz or 24000 motor signals per minute to be precise. Multicopters also have 6 degrees of freedom. Some drones like racing and freestyle drones can flip entirely as well as perform extreme maneuverers with ease due to this freedom. Hence there is a need to control each degree of freedom individually as well their overall vector effect on the copter.

Due to this complexity, it is required to run 2 different control loops, namely outer loop and the inner loop. The outer loop is responsible for the position and attitude control

of the copter in the x, y, and z axes. And the inner loop is responsible for the angular orientation and attitude of the drone in the roll, pitch, and yaw axes. By separating the linear and angular control systems it's easier for the drone to now stabilize itself in the sky with a few sensors like accelerometers, IMUs, gyroscopes, magnetometers, and barometers to name a few.

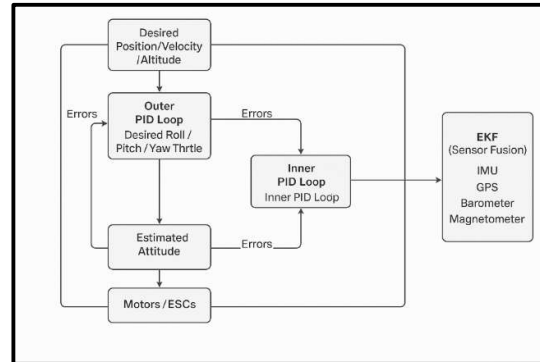


Fig 7: Block diagram of the control flow of the signals from the outer loop to the inner loop and finally to the motor ESCs

The outer loop is like a master loop whose goal is to correct the drone's position in x, y and z axes. It produces the required roll, pitch and yaw values to correct the position of the drone and sends these values as input to the inner loop. It takes EKF values from sensors like GPS, barometer, optical flow sensors and more to know its current position and produces the desired throttle, roll, pitch and yaw values needed to bring the drone to the required state using a PID control algorithm.

The inner loop is core loop which actually controls the motion of the drone. A copter essential moves by controlling its angular movement in all the axes and controlling the throttle. So, this loop acts like the control linkages on an aircraft. It takes the values of the required roll, pitch, yaw and throttle and produces the actual motor control signal values that makes the copter perform the exact action in the very smooth and precise fashion.

4.2. PID and EKF algorithms

As discussed earlier for a multicopter to fly it requires to run two control loops both of which are depended on the PID and EKF algorithms to perform its specific goal. Here, EKF is acts as an input algorithm and PID acts as an output algorithm. EKF or Extended Karman Filter is basically an algorithm that combines different noisy sensor values to estimate the true value of attitude, position and velocity of the drone. While, PID or Proportional Integral Derivate is a very popular control algorithm in robotics which

essentially tries to reduce the error between the current state and desired state continuously, which correction of attitude, position and velocity of the drone.

PID or Proportional Integral Derivate controller calculates the error difference and correction rate using mainly four components. They are error, proportional gain, integral gain, and derivate gain.

$$u(t) = K_p e(t) + K_i \int_0^t e(t) dt + K_d \frac{de(t)}{dt}$$

where,

$e(t)$ = error = desired – measured

K_p = proportional gain

K_i = integral gain

K_d = derivate gain

$u(t)$ = control output (motors thrusts)

Here, proportional ($K_p.e(t)$) is the immediate error correction for a larger error correction which requires immediate and higher correction value. Integral ($K_i \int e(t) dt$) fixes the long-term accumulated errors like GPS drift. And finally derivate ($K_d(de(t)/dt)$) is component that predicts the future and smoothens the response preventing oscillations and overshooting.

In a Pixhawk PID runs in three different stages. First is the angular rate control which is the fastest about 400-800 Hz and it controls how fast the drone rotates. Next is the attitude control with a speed of about 100-200 Hz which controls the angle of the drone in roll rates, pitch rates and yaw rates. And lastly it is position control PID that controls the x, y and z position of the drone based on GPS signal and sets the desired tilt angles typically at a speed of 50-100 Hz.

EKF is a state estimator that predicts and corrects the drone's understanding of itself. It fuses noisy and messy sensor data into a clean estimate of position, attitude, and velocity. It runs in two steps. First is the prediction step which predicts the new state based on the last state and control inputs. Second step is the correction step which corrects the prediction using the sensor measurements. Pixhawk uses a version of EKF called EKF2 or EKF3 which corrects the values of position, velocity and angles using GPS position, barometer altitude, magnetometer heading, and accelerometer attitude.

4.3. Motor Mixing for Coaxial Quad

Motor mixing is the logic that tells how fast which motor should spin to achieve desired throttle, pitch, roll, and yaw based on RC inputs or autopilot inputs. In a coaxial quad there are two motors on each arm, one above the other spinning in opposite directions. It's usually used when higher thrust is required and space is less. In a Pixhawk controller the motors are controlled by giving a label to each motor which is specific for each type of motor configuration. In this case there are 8 motors hence each motor is labelled with a number from 1 to 8. In our case are using the X8 motor labelling because though it is a H-frame our motors are placed in equidistant fashion from the centre just like an X-frame for increased agility. Here is a diagram and table for the labelling of the motors.

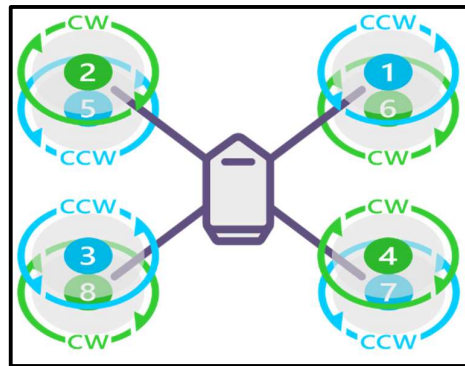


Fig 8: Motor configuration diagram showing the X8 motor labelling

Motor Label	Location	Direction
1	Front Right Top	CCW
2	Front Left Top	CW
3	Rear Left Top	CCW
4	Rear Right Top	CW
5	Front Left Bottom	CCW
6	Front Right Bottom	CW
7	Rear Right Bottom	CCW
8	Rear Left Bottom	CW

Table 3: Table presenting the motor labels and its respective directions for an X8 configuration drone

Here CW means Clockwise and CCW means Counter Clockwise. This motor configuration preserves the torque balance as every clockwise motor has a counter clockwise partner.

Arducopter uses a table called a motor mixing matrix to refer to for control. The matrix gives the information for which motor performs what movement when its speed is

increased. Using this matrix table arducopter can change the speed of the motor accordingly to achieve the desired movement like roll, pitch, yaw or throttle.

Motor	Throttle	Roll	Pitch	Yaw
1	+1.0	+1.0	-1.0	+1.0
2	+1.0	-1.0	-1.0	-1.0
3	+1.0	-1.0	+1.0	+1.0
4	+1.0	+1.0	+1.0	-1.0
5	+1.0	-1.0	-1.0	+1.0
6	+1.0	+1.0	-1.0	-1.0
7	+1.0	+1.0	+1.0	+1.0
8	+1.0	-1.0	+1.0	-1.0

Table 4: Table presenting the motor mixing matrix for an X8 configuration drone

Here the values in the table follow the signage based on the standard aerospace coordinate system NED (North-East-Down), which gives the direction of the positive pitch as forward, positive roll as right and positive yaw as clockwise rotation as shown in the diagram below.

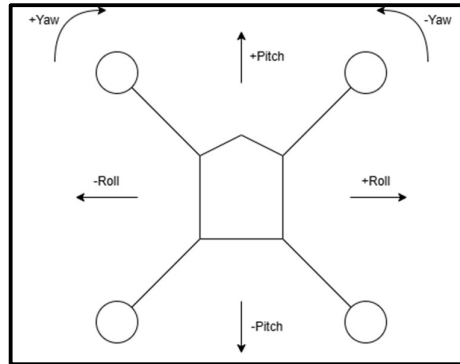


Fig 9: Image representing the NED directions in multicopter

4.4. Hardware and software description

The Pixhawk 2.4.8 flight controller, a trusted platform widely used in UAVs for flight and robotic arm control, serves as the central component of the H-Frame drone system. This advanced flight controller, powered by ArduCopter software, ensures smooth integration with multiple components and offers flexibility in development. The system benefits from PID tuning, allowing precise adjustments for flight stability and robotic arm control, which is essential for high-rise cleaning tasks. Additionally, LUA scripting is utilized to enable specialized control functions, optimizing performance for tasks such as solar panel and glass facade cleaning.

4.4.1. Hardware Components

The drone is designed using high-performance components and lightweight, durable materials to ensure stable and reliable operation under various environmental conditions.

Hardware	Specifications
Flight Controller	Pixhawk 2.4.8
Motor	FlyCat 5010 360kV 2s-6s
ESC	Hobbywing XRotor 50A 4s-6s
Propellor	14-inch Carbon Fibre
Motor Configuration	Coaxial Configuration
Sprayer Pump	Diaphragm Pump
Flow Rate	5L/min @ 14s
Battery	6s 6800mAh Lipo
Servos	MG995 180 degree
Microcontroller	Arduino Nano
Main Frame Tubes	Square Carbon Fibre 20mm
Landing Gear	Round Carbon Fibre 20mm
GPS Module	Here 3+
Structural Mounts	3D Printed ABS and PETG
Pixhawk Mount	3D Printed PLA
Telemetry Module	SiK Holybro Telemetry 100mW
Receiver	TBS Crossfire Micro
Transmitter	Radiomaster TX16s

Table 5: Table stating the major hardware components used the prototype UAV system

4.4.2. Software Tools

Before building the drone, we require to design a CAD Model of the done to validate the planned design and specifications. It not only gives an idea of how the prototype will look like but also give all information of the tolerances and also helps in checking for the 3D printed have proper tolerances before printing. We used Autodesk Fusion 360 for designing CAD model of the prototype as it's a cloud-based software with simple tools and huge community support for designing.



Fig 10: Screenshot of the HUD and map display of the mission planner software

For programming the firmware of the autopilot, we are using mission planner software to flash and setup arducopter firmware into the Pixhawk flight controller. Mission planner is one the best open-source ground control software which is designed for flight controllers like Pixhawk. They have a very good HUD with instrument gauges giving real time information of the flight as well as option to plan an autonomous mission. It connects to the drone via the telemetry module through a USB port. With the telemetry module we are using we can communicate up to 3kms. It's used to monitor the flights in real time acts a secondary safety control in case the radio controller of the remote pilot fails.

4.5. Key Specifications

The H-frame drone, powered by a 6S 6800mAh LiPo battery, offers an efficient and powerful solution for high-rise building and solar panel cleaning. With a rigid and lightweight carbon fibre frame, this design ensures durability, stability, and optimal performance under demanding conditions. Here the specifications are listed in a tabular column.

Parameter	Specifications
Frame Size	640mm (L) x 640mm (W) x 300mm (H)
Carbon Fibre Tubes (Sq.)	20mm x 18mm
Carbon Fibre Tubes (Rd.)	20mm x 18mm
Propulsion System	8 x BLDC motors
Motor kV Rating	360kV
Propellers	8 x Carbon Fibre 14 inch
Battery Chemistry	Lithium Polymer
Operating Voltage	25.2V
Remote Controller Range	24 kms (LOS)
Remote Controller Frequency	2.4 GHz

Telemetry Module Frequency	433 MHz
Telemetry Module Range	500m
Empty Weight	3.5 kgs
Fully Loaded Weight	7 kgs
Max Thrust Produced	10 kgs
Thrust to Weight Ratio	1.4:1
Tank Capacity	1 Litre
Pump Flow Rate	5L/min @ 58.8
Total Flight Time	5-6 mins

Table 6: Table summarising the key specifications of the UAV system

4.6. Sprayer System

Based on the mission requirement a sprayer system was to be designed that could effectively sprayer and clean surfaces like walls, solar panels, and glass facades without damaging the surface being cleaned. It was also noted that the system should able to cover as much as area as possible in order to be more efficient in cleaning.

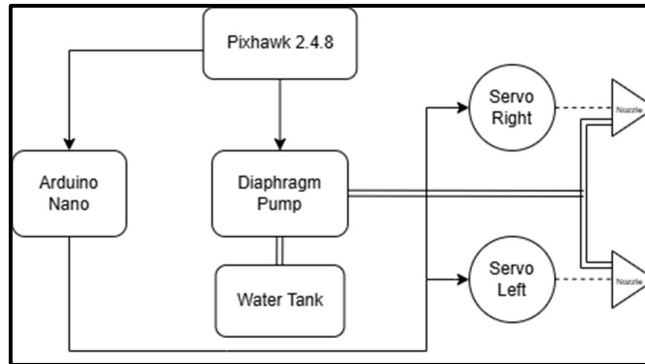


Fig 11: Block diagram showing the control flow of the sprayer system

The system consists of a Hobbywing Diaphragm pump which can pumps the water from the water tank to the two nozzles which are mounted on the servos which move 45 degrees each to cover a wider area and perform an effective spray. The diaphragm pump takes the signal from the radio controller via the Pixhawk to spray. Diaphragm pumps work by using a flexible diaphragm to create alternating pressure and suction, drawing and discharging the fluid. This mechanism allows to create a very high-pressure system which also very light weight compared to similar pressure pump. Hence, it's a first choice when it comes to drones with sprayer applications.

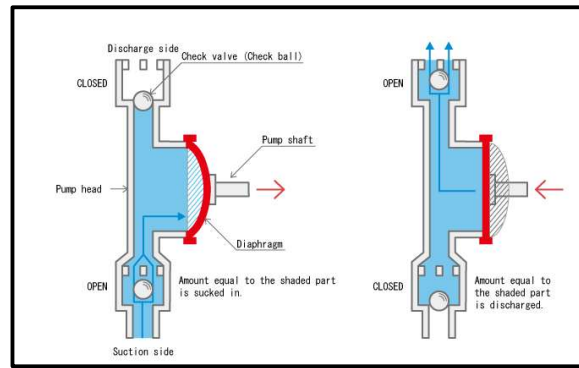


Fig 12: Image showing the working of a classical diaphragm pump

Above is a diagram showing the working of the diaphragm pump when in when the water is sucked outlet check value closes and inlet check valve opens pulling in the fluid. Then when the diaphragm is compressed, the fluid is pushed creating due to which the inlet check-value closes and outlet check value opens pumping the fluid out with higher pressure.

4.7. Power and Electronic Speed Control:

The drone gets its power a Lithium Polymer Battery which have capacity of 6.8Ah and a full charge voltage of 25.2V. The reason to use a Lithium Polymer battery is because of is high discharge rate and higher charge density. The power distributed via a power distribution module which sends 5V for the Pixhawk and the Arduino Nano and 25V for the motors and the pump. Choice for the battery is based on the operating voltage of the motor, required capacity for the flight time, and weight of the battery. Here is a power flow diagram.

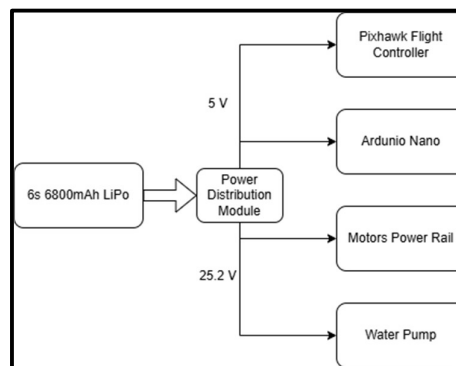


Fig 13: Block diagram showing the flow of electrical power in the UAV system

The battery size was calculated based on a required flight time of 7-8 minutes under fully loaded condition. This requirement was decided based on the real-life mission which involves different phases of the flight such as take-off, climbing, approach and adjust, spraying and cleaning, then descending and landing. As well there should be a certain

buffer time in case of any less-than-ideal weather conditions or issues during landing which require a little extra hover time. Considering these phases, a flight of about 7-8 minutes was estimated but due some inefficiencies the real-life flight time achieved about 5-6 minutes which is still good enough for the operations of the drone but these aerodynamic inefficiencies could be addressed in the future.

To know which battery size is suitable and the approximate flight time we will get out of we can perform some calculations. First, we need to know the maximum amount of current the drone will consume and what is its average current consumption during hover. To do this we consider per motor current consumption in both scenarios and multiple it with the number of motors, plus the current consumed by the sprayer system and other systems.

$$\text{Max current per motor } (C_m) = 25A$$

$$\text{Total Max current of all motors } (I) = 25A \times 8 = 200A$$

$$\text{Max current of Spayer system } (C_s) = 12A$$

$$\text{Total Current Consumed max} = 200 + 12 = 212A$$

The continues current by a battery should be more than 215A for safety and the continuous current given by our chosen battery is given by

$$\text{Continuous Discharge Current} = 6.8A \times 40 = 272A$$

which is less than the total max current consumed hence it is considered safe to fly.

Parameter	Specification
Battery Chemistry	Lithium Polymer
No. of Cells	6s
Capacity	6800 mAh
Nominal Voltage	22.2 V
Full Charge Voltage	25.2 V
Full Discharge Voltage	19.8 V
Storage Charge Voltage	22.8 V
C Rating	40C/80C
Continuous Discharge Current	272 A
Peak Discharge Current	544 A
Stored Power	150 W
Weight	800g
Power Consumption (No Payload)	640 W
Power Consumption (Full Payload)	1200 W

Flight Time (No Payload)	12 minutes
Flight Time (With Payload)	6 minutes

Table 7: Table summarizing the UAVs power system parameters

4.8. Communication and Control:

The drone is primarily communicated with the remote controller by the pilot but it also has a secondary communication system with a ground control station for redundancy. While the cleaning operations can be only performed by the pilot the ground control station can perform tasks GPS based waypoint navigation, return-to-home, auto landing as well as give the live status of the drone like AHRS data, GPS location, number of satellites connected, battery voltage and much more.

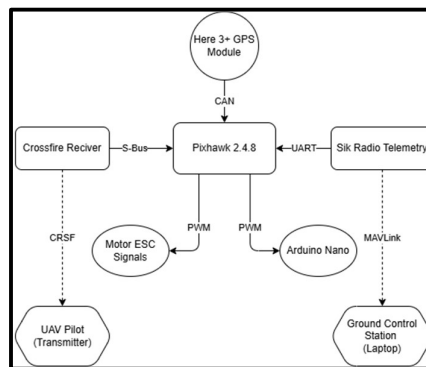


Fig 14: Block diagram showing the working of the communication system of the UAV

There are two types of communication that is occurring here. One is on board the drone which is in a wired form and another is from the ground to the drone which is in wireless form. Onboard the drone the communication protocol is different for different devices for example, the GPS Module communicates in CAN protocol, and the motor ESCs, Arduino nano gets PWM inputs from Pixhawk, the telemetry module connects to the UART port of the Pixhawk and finally the crossfire receiver sends PPM signals to the Pixhawk through S-Bus interface.

The wireless communication between the transmitter and the receiver on board the drone occurs wirelessly in 915 MHz frequency. It uses a proprietary protocol called CRSF which is specifically design for long range communication with a range of up to 24 kms. The power levels of the systems are 250mW both on the ground as well on board. While that is the case for the control signals from the pilot the ground operator connects the laptop running a GCS software like Mission Planner or QGround Control via the SiK telemetry module which talks in 433 MHz frequency giving better weather penetration and a range of 5 kms. The power levels of this system on both the ground as well as on the drone is

about 100mW and uses MAVlink protocol which establishes a PPP (Point-to-Point) link between the two telemetry modules.

Here is a table summarizing the specifications of the communication system.

Parameter	Specification
Here 3+ GPS Interface	CAN Port
GPS Module Protocol	DroneCAN Protocol
GPS CAN Speed	8 Mbit/s
Motor ESC Interface	Main PWM Pins
Motor ESC Input Signals	PWM Signals
Pump Interface	Aux PWM Pins
Pump Input Signals	PWM Signals
Crossfire Receiver (Pixhawk)	S-Bus
Crossfire Receiver Signals (Pixhawk)	PPM
Crossfire Receiver Protocol (Transmitter)	CRSF
Crossfire Receiver Type	Micro
Transmitter	TX16s with CRSF Micro Module
CRSF link frequency	915 MHz
Receiver Power Level	250mW
Transmitter Power Level	250mW
Crossfire System Range	24 kms
Telemetry Module Interface (Pixhawk)	UART
Telemetry Module Protocol (Ground)	MAVLink
Telemetry link frequency	433 MHz
Telemetry Module Type	Holybro Sik Radio Telemetry
Ground Telemetry Module Power Level	100mW
On Board Telemetry Module Power Level	100mW
Telemetry System Range	5 kms

Table 8: Table summarizing the communication system of the drone

Chapter 5: Results and Analysis

In this chapter, we will be presenting the experimental results obtained from the prototype of the drone. It will be followed by discussion of interpreting the findings with reference to the project objectives and literature. The evaluation focus on flight stability, payload capacity, cleaning effectiveness and efficiency of the drone system. The drone was tested using both autonomous as well as manual flights to eliminate the human bias in the results. The drone was tested for hover flight stability, agility, and ability to withstand winds as well as easy of operation for cleaning.

5.1. Autonomous Flight

In the autonomous flight, the test criteria were to test the stability of the drone in hover and the battery lifespan of the drone. A total of three flights were completed one without payload, one with the sprayer system attached and finally one with the filled tank. This was done to test how stable the drone is with increasing weight in the system. Generally, higher the load less the stability as the drone loses its ability to counter act any imbalance. This is amplified as the loading is increased as to counter act the excess load more power is needed but less power is available for counter action as the load increases and more is used up just to lift the drone in the air.

The flight was basically a GPS based mission to hover the drone for over 15 minutes and land the drone when the battery failsafe triggers. The mission was designed and uploaded to the drone using the QGroundControl Software. GPS based missions are very accurate and are best for flying missions that are flown in open fields as its simple and easy to setup.

Firstly, a fence was setup which was about 50m by 50m in length and width which is bit less than the football field we were flying the craft in. The fence prevents the drone from flying out of a safe area and in case breached by mistake it can land it safely. Then the mission was setup with a take-off command and then hovering at 3m AGL (Above Ground Level) for over 15mins and then land in the same spot. The idea was that the drone's calculated endurance is below 13 mins which should make the drone Autoland in battery failsafe mode giving us an idea about the flight time of the drone.

During the first mission the drone perform excellently showing the best stability and staying spot on with only very minor drifts which is well within the limits of a GPS based mission without precession RTK base station setup. The drone even was able to maintain its GPS location when the winds picked up and titling the drone into the crosswind

showing excellent stability characteristics. The drone flew for a total of 12 mins after which the battery failsafe was triggered and the drone performed a safe auto land.

In the second mission the drone was able to take-off perfectly with the sprayer system fully attached but without the water loaded. The drone was able to maintain a stable hover but had drifts much more than previous flight and faced a bit difficulty to maintain its position to crosswinds or sudden gusts. It took longer for the drone to adjust when there was any sudden gust of the wind. This shows the agility of the drone is reduced by the weight of the sprayer system. Still the drifts were within the acceptable limits. It was able to fly for a total of 6 minutes.

Last flight was with the water filled fully in the tank. This was done as a separate trial as liquids have a tendency to cause sloshing effect when moved which can cause a dynamic CG shift which can send the drone into oscillations and worse cases can potentially lead to a crash. Because of this we had added baffles and made sections within our tank which should prevent such a situation. During the flight the drone did show signs of struggle in terms of agility as it was reaching its limit of payload carrying capacity. Still the drone did not go into any sort of oscillations and was fully stable. It was able to fly for a total of 5 minutes.

Here is a table summarizing the results of the autonomous flights. Points have been awarded based on factors like stability, agility and flight time where 5 means highest and 0 means the least.

Parameter	No Payload	With Sprayer System	With Filled Tank
Stability	4.8 au	4.2 au	3.8 au
Agility	4.8 au	3.5 au	3 au
Flight Time	4 au	2 au	1.6 au

Table 9: Table showing the results of the three autonomous flights

Here the flight time is considered as 5 points if it achieves a flight of 15 minutes.

5.2. Sprayer System Tests

Before going for the manual flight tests ground tests were completed on the sprayer system using the onboard tank as well as an external tank. This was done to test how well the system works in terms of cleaning effectiveness, reliability of the mechanism and overall functioning of the system. In both cases the system was powered and controlled using the onboard battery and control systems in order to mimic a real-world flight. Ground

tests also give a long testing time that a flight test helping detect any problems that would occur over time in the system.

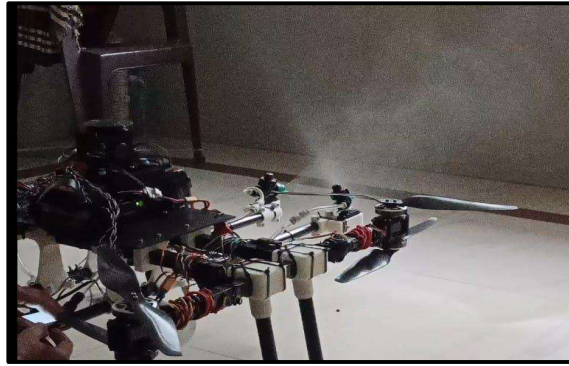


Fig 15: Image showing the initial testing of the sprayer system on the ground

First test was with an external tank with which a bucket of water of about 10 litres. The system was run and tested for leaks in the system as well as if the servos are able to handle the load for such a long time. The servos showed no signs of stress or heating as well as the vibrations of the motor was also dampened by the installed dampeners. The system ran for about 8 – 10 minutes continuously and this was repeated two more times just to confirm the reliability of the system. Next, it was tested with the onboard tank which ran only for about 1 minute before the tank ran out of water. No leaks were detected in the system hence it was considered safe for flight test ensuring that no water entered any electrical part.

5.3. Manual Flight

Since the system is meant to be flown manually during operations it should be tested manually for stability and ease of control of the drone. The manual flight test was conducted in both the conditions with sprayer and without sprayer. Factors like throttle value, drifting of the drone, stability, agility and ease of control were tested. During the flight test the pilots were also changed to remove any bias of one pilot and results were inferred based on that.

For the first manual flight the drone was flown in stabilize mode which is fully manual control mode of the drone. Two flights were conducted by two different pilots and each flight lasted for about 90 seconds. This was done without the payload and factors like stability and agility were reported by the pilots. The pilots found the drone to be stable as well as agile for such a large drone and very able to easily perform coordinated turns and emergency braking with ease. The drone reportedly was able to take-off at 50-55% throttle value which suggests a very well-balanced drone control.

Next set of flights was conducted in altitude hold mode which can help detect drifts in roll, pitch and yaw while eliminating the issue of altitude drift with the throttle control.

taken over by the drone. In this mode as well both the pilots reported the drift to be extremely minimum and said they could fly the drone stick free for a short while, that is, that drone even without GPS support under calm winds could maintain its position in the air which shows good tuning of the drone's controls.



Fig 16: Image showing the drone performing a manual cleaning operation on a window

The last test flights were the actual operation of cleaning a building. This was done in stabilized mode as well as altitude hold mode, and test lasted for about 90 secs each which included take-off, climb, approaching the target and then spraying the window and then returning and performing a safe landing. The pilots reported the drone in agility as expected from the previous autonomous tests and they could feel the drone working hard to carry the weight of the sprayer system. The take-off and hover throttle value were observed to be about 60-65% and the drone was still controllable and the pilots were able to successfully clean the window with ease and effectiveness.

The results are summarized in the table below. Here the ratings were reported by the two remote pilots who flew the drone in the same conditions. The different ratings were collected in order to reduce any human bias by a single pilot and shows little variance between the ratings of the two pilots. It follows the same rating system where 5 points means best while 0 means least.

Parameter	Stabilized Mode (No Payload)	Altitude Hold Mode (No Payload)	Stabilized Mode (With Payload)	Altitude Hold Mode (With Payload)
Stability	4.7 au	4.9 au	3.8 au	4.1 au
Throttle Value	52%	-	63%	-
Agility	4.8 au	4.2 au	3.5 au	3.2 au
Drifting	4.2 au	4.9 au	3.8 au	4.5 au
Cleaning effectiveness	-	-	3.8 au	4 au

Table 10: Table showing the manual flight test results by Pilot 1

Parameter	Stabilized Mode (No Payload)	Altitude Hold Mode (No Payload)	Stabilized Mode (With Payload)	Altitude Hold Mode (With Payload)
Stability	4.8 au	5 au	3.7 au	4.3 au
Throttle Value	54%	-	61%	-
Agility	4.6 au	4.4 au	3.3 au	3 au
Drifting	4 au	4.8 au	3.4 au	3.8 au
Cleaning effectiveness	-	-	3.6 au	3.8 au

Table 11: Table showing manual flight test results by Pilot 2

5.4. Final Inference

After all the ground test and flight test both autonomous and manual flight we can infer from the results that the drone is able to satisfy our initial objectives and is suitable to perform cleaning tasks. Based on the tests that drone have a very good stability rating does not show any kind of oscillations during flight. There is minor drifting with the payload and this is due to wind and other external factors which is not under our control.

Also, the copter still can be further turned using PID tuning tools to increase its agility as well as stability when it is fully loaded. This will also help during autonomous flights as the drone still drifts a bit when on full autonomous mode.

The cleaning effectiveness is satisfactory enough to prove the technology can be used with more improvements to both the sprayer system such as using a tethered water supply as the time of only 1 minute for the tank is too less for an effective clean. Based on these results we can infer that this technology could be useful in the real-world scenario for actual cleaning of buildings and solar panels with automation and tethered power and water supply integrated to the drone.

Parameter	Value
Frame Type	H-Frame
Configuration	Co-axial Quad (X8)
Dry Weight	3.5 kgs
Sprayer System Weight	3.5 kgs
Total Weight	7 kgs
Flight Time (No payload)	12 minutes
Flight Time (Full Load)	5 minutes

Tank Capacity	1 Litre
Cleaning Time	1 minute
Pump Type	Diaphragm Pump
Pump Capacity	5L/min @ 14s (58.8V)
Operating Voltage	6s (25.2V)
Max Current Draw	220A
ESC Current Rating	50A
Battery	6s 6800mAh
Max Service Ceiling	50m
Operational Ceiling	10m
Max Speed	5m/s
Operational Ceiling	1m/s

Table 12: Table showing the final inference of the result analysis

5.5. Flight Logs

The flight logs taken during the drone's testing phase offer important information on its stability, performance, and accuracy of navigation in the actual world. Telemetry information gathered from the GPS module and onboard flight controller during test flights was used to create these records. The reliability of the drone's locating system, altitude hold capabilities, and general flight characteristics are all confirmed by the examination of these records. The following figures provide a detailed discussion of the outcomes derived from the logged data.

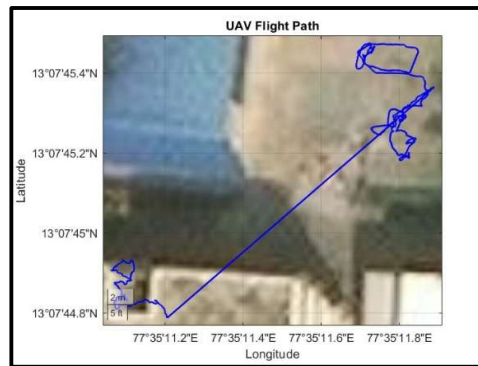


Fig 17: Graph showing the UAV's flight path acquired from the GPS data where x-axis is the latitude and y-axis is the longitude with a google earth 2D image overlayed in the background for easier referencing

The drone's fly route throughout the specified test region is highlighted by the recorded coordinates, which show its spatial trajectory. According to the data, there was little drift and departure from the planned flight path, and the drone maintained constant

positional accuracy. This illustrates how well the GPS module works to give the flight controller real-time location feedback, which is essential for tasks including waypoint-based navigation and stable hovering. When flying close to delicate infrastructure, such as solar panels or building facades, the drone's ability to respond consistently to pilot commands and sustain controlled lateral movements is also reflected in the trajectory pattern.

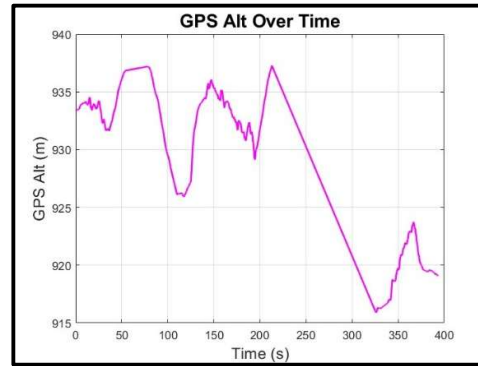


Fig 18: Graph of GPS altitude data in meters (x-axis) plotted over time in seconds (y-axis) showing the change in altitude during the flight

The climb and descent profiles, as well as areas of consistent altitude hold, are clearly shown on the graph. The drone's barometer and GPS-based altitude estimate systems operated effectively in tandem with the control algorithms, as seen by the smoothness of the altitude curve. As a result, there was little oscillation or variation when the drone reached and maintained its target altitudes. For jobs like surface cleaning, where keeping a steady height in relation to the cleaning surface enables continuous operation, stable altitude hold is extremely important. Additionally, the data confirms that even with the payload (cleaning mechanism) attached, the propulsion system and control loop can efficiently balance weight and thrust.

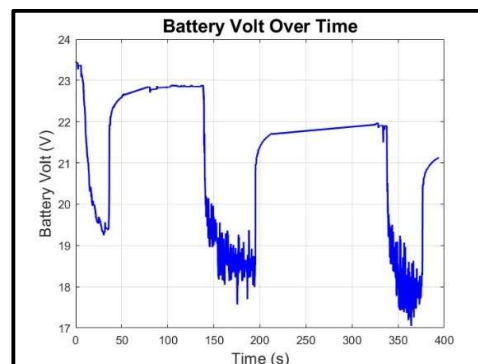


Fig 19: Graph showing the change in measured battery voltage in volts (x-axis) over time in seconds (y-axis) during the flight indicating consistent drop of voltage over time

As the flight continues, a steady drop in voltage is seen, which is to be expected given the propulsion system's and the onboard electronics' constant power consumption.

Crucially, there are no abrupt voltage reductions or spikes, which suggests a consistent power delivery and a healthy battery discharge profile. In order to guarantee safe operation, avoid mid-air shutdowns, and maximize endurance—especially when using auxiliary payloads like the cleaning mechanism—it is imperative to monitor battery voltage while in flight.

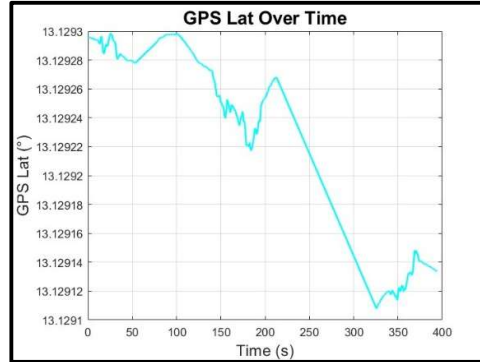


Fig 20: Graph of GPS latitude data in degrees (x-axis) plotted over time in seconds (y-axis) showing the change in latitude during the flight

As the drone travelled along its flight path, the graph displays the change in latitude. The data's steady and upward trend indicates that positional movement along the north-south axis was accurately recorded. For applications that need precise geographic placement, this is essential. Additionally, the latitude data's consistency supports the previously described GPS performance, confirming that the drone's spatial awareness and navigational dependability were maintained throughout the test flights.

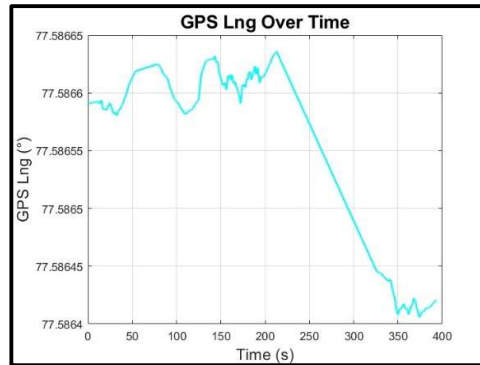


Fig 21: Graph of GPS longitude data in degrees (x-axis) plotted over time in seconds (y-axis) showing the change in longitude during the flight

This data shows steady tracking of the drone's position, much as the latitude graph. The drone's GPS module successfully recorded geographical alterations, as seen by the crisp variation in longitude readings. This is crucial for mapping, waypoint navigation, and carrying out location-specific cleaning tasks. The drone's position may be reliably traced throughout its mission profile because to the combination of latitude and longitude data.

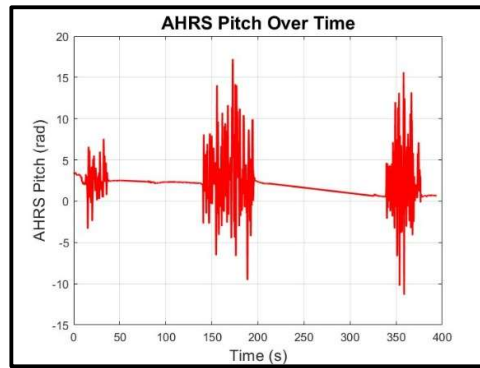


Fig 22: A graph showing the pitch angle in degrees (x-axis) against time in seconds (y-axis) indicating the attitude of drone in the pitch axis for the entire flight

The drone's nose-up and nose-down positions are represented by its pitch. The drone's forward and backward tilt adjustments in response to pilot commands and ambient factors are depicted in the graph. The flight control system successfully stabilized pitch during manoeuvres and hovering, as evidenced by the seamless transitions and absence of sudden oscillations. During cleaning operations, controlled pitch behaviour is necessary for steady forward motion and accurate approach toward vertical surfaces.

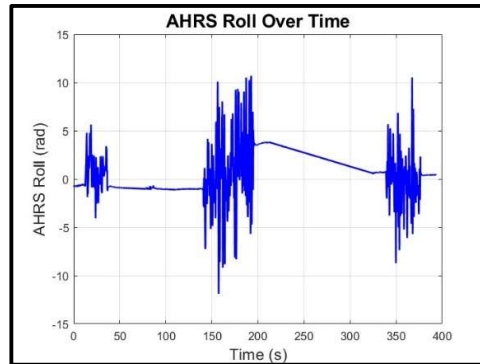


Fig 23: A graph showing the roll angles in degrees (x-axis) against time in seconds (y-axis) indicating the roll attitude of the drone for the duration of the flight

Controlled roll behaviour with progressive fluctuations that correspond to lateral movements during flight is demonstrated by the data. A crucial performance indicator is consistent roll stability, particularly in close-quarters tasks like cleaning buildings or solar panels where accuracy is needed. The graph demonstrates that the drone successfully maintained lateral balance and reacted to control commands in a predictable manner.

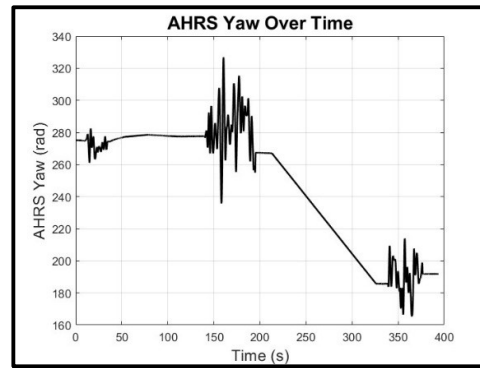


Fig 24: Graph showing the yaw rotations performed in degrees (x-axis) over time in seconds (y-axis) during the test flight of the drone

The drone's rotation to alter its flight path during tests is reflected in the observed yaw variation. The drone's ability to execute manoeuvres and retain heading stability without unpredictable rotations is suggested by the smooth yaw shifts. For safe navigation in limited spaces, alignment over target surfaces, and directional corrections, controlled yaw movements are essential.

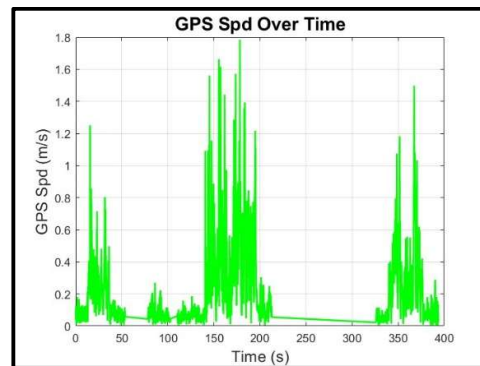


Fig 25: Graph showing the indicated air speed of the drone in meters per second (x-axis) to the event time in seconds (y-axis) during the test flight of the drone

The drone's ability to accelerate, decelerate, and maintain steady velocity during various flying phases is shown in the graph. A well-balanced thrust-to-weight ratio and effective propulsion system performance are demonstrated by the smooth and predictable speed variation that is seen. When working close to delicate surfaces, maintaining the proper pace is crucial for both safe navigation and efficient cleaning.

The operational stability and design efficacy of the drone are confirmed by the thorough examination of flight log data, which includes location, altitude, orientation, speed, and power parameters. The designed drone can perform controlled, dependable flights and effectively complete its specified cleaning tasks, as confirmed by the smooth trends seen across all metrics. Additionally, these recorded outcomes provide important proof of system resilience, which is essential for practical implementation in infrastructure maintenance situations.

Chapter 6: Conclusion and Future Scope

The conclusion of this research emphasizes the significant advancements made in the development of the H-Frame drone, designed specifically for cleaning solar panels and high-rise buildings. By effectively addressing key challenges like stability, payload capacity, and manoeuvrability, cleaning effectiveness this project highlights how the H-Frame design offers a solution to risky and tedious task of infrastructure maintenance. The research demonstrates a 7 kg UAV system which can carry a load of up to 3.5 kgs and is able to fly with good stability in autonomous and manual control and perform the task of cleaning of building facades.

The drone was able to complete a mission of cleaning a window and demonstrated an endurance of 5-6 minutes which was deemed sufficient for based on the size of the tank used in the drone. The cleaning effectiveness of the drone was found to be moderate at best reflecting the prototype nature of the sprayer system, the primary objective of demonstrating the technology feasibility of an aerial maintenance vehicle was achieved successfully. The potential of such drone to enhance the efficiency and safety of cleaning operations in challenging environments, especially in high-altitude conditions. Future work could focus on further optimizing the drone's autonomous capabilities and expanding its range of applications across industries. The outcome of this project contributes valuable insights into the evolving field of autonomous drones and their integration into real-world maintenance tasks, paving the way for more sustainable and cost-effective solutions in infrastructure and renewable energy sectors.

6.1. Future Scope

While the project has achieved significant progress, there still some limitations which can be focused on refining and expanding the drone's capabilities to ensure optimal performance for its intended cleaning tasks. The cleaning effectiveness of current prototype is moderate at best. Better cleaning solution like higher pressure pumps, robotic arms to reach hard to access areas and using better cleaning agents other than water can help improve the effectiveness of the system significantly.

The project will transition towards implementing autonomous functionalities, including programming predefined flight paths tailored to specific cleaning tasks and integrating sensors for obstacle detection and avoidance. Autonomous operation will reduce the need for manual control, enabling the drone to perform cleaning tasks efficiently and reliably with minimal human intervention. This will also open up the opportunity to

integrate swarm drone technology and scale up the operation to increase efficiency and reduce time significantly for large building and solar farms.

Subsequently explore tethered power and water supply from the ground can be explored which will allow the drone to perform operations for a few hours instead of a few minutes extending its capability. These enhancements aim to revolutionize maintenance tasks by combining safety, efficiency, and cutting-edge technology to overcome conventional limitations of battery and carrying an onboard tank.

By addressing these areas, the H-Frame drone will evolve into a fully functional and efficient cleaning platform. These developments aim to meet the project's ultimate objectives: providing a stable, reliable, and autonomous solution for cleaning solar panels and high-rise structures. The enhanced system will not only improve operational efficiency but also contribute to safer and more effective cleaning methods in challenging environments.

Bibliography

- [1] L. A. Al-Haddad *et al.*, “Quadcopter Unmanned Aerial Vehicle Structural Design Using an Integrated Approach of Topology Optimization and Additive Manufacturing,” *Designs (Basel)*, vol. 8, no. 3, Jun. 2024, doi: 10.3390/designs8030058.
- [2] A. Ollero, M. Tognon, A. Suarez, D. Lee, and A. Franchi, “Past, Present, and Future of Aerial Robotic Manipulators,” *IEEE Transactions on Robotics*, vol. 38, no. 1, pp. 626–645, Feb. 2022, doi: 10.1109/TRO.2021.3084395.
- [3] A. Suarez, V. M. Vega, M. Fernandez, G. Heredia, and A. Ollero, “Benchmarks for Aerial Manipulation,” *IEEE Robot Autom Lett*, vol. 5, no. 2, pp. 2650–2657, Apr. 2020, doi: 10.1109/LRA.2020.2972870.
- [4] R. Arifuddin, R. U. Latief, and A. Suraji, “An investigation of fall accident in a high-rise building project,” in *IOP Conference Series: Earth and Environmental Science*, Institute of Physics Publishing, Feb. 2020. doi: 10.1088/1755-1315/419/1/012144.
- [5] A. Al Hulaibi, H. Wahid, S. Al Saif, J. Sadeq, S. Esmaili, and M. Kandil, “SkyBot - A Novel Autonomous Window Cleaning Drone,” in *4th International Conference on Electrical, Communication and Computer Engineering, ICECCE 2023*, Institute of Electrical and Electronics Engineers Inc., 2023. doi: 10.1109/ICECCE61019.2023.10442126.
- [6] I. Abuzayed, A. Rahman Itani, A. Ahmed, M. Alkharaz, M. A. Jaradat, and L. Romdhane, “Design of Lightweight Aerial Manipulator With a CoG Compensation Mechanism,” 2020.
- [7] W. Thomas, P. Wegrowski, J. Lemirick, and T. Deemyad, “Lightweight Foldable Robotic Arm for Drones,” in *2022 Intermountain Engineering, Technology and Computing, IETC 2022*, Institute of Electrical and Electronics Engineers Inc., 2022. doi: 10.1109/IETC54973.2022.9796899.
- [8] W. Walendziuk, P. Falkowski, and K. Kulikowski, “The Analysis of Power Supply Topologies for Tethered Drone Applications,” MDPI AG, Aug. 2020, p. 25. doi: 10.3390/proceedings2020051025.
- [9] J. Li and F. Janabi-Sharifi, “Public Opinion About the Benefit, Risk, and Acceptance of Aerial Manipulation Systems,” *IEEE Trans Hum Mach Syst*, vol. 52, no. 5, pp. 1069–1085, Oct. 2022, doi: 10.1109/THMS.2022.3164775.
- [10] M. Alkaddour *et al.*, “Novel Design of Lightweight Aerial Manipulator for Solar Panel Cleaning Applications,” *IEEE Access*, vol. 11, pp. 111178–111199, Oct. 2023, doi: 10.1109/ACCESS.2023.3321859.
- [11] D. Lee, H. Seo, I. Jang, S. J. Lee, and H. J. Kim, “Aerial Manipulator Pushing a Movable Structure Using a DOB-Based Robust Controller,” *IEEE Robot Autom Lett*, vol. 6, no. 2, pp. 723–730, Apr. 2021, doi: 10.1109/LRA.2020.3047779.
- [12] B. E. Y. Belmekki and M. S. Alouini, “Unleashing the Potential of Networked Tethered Flying Platforms: Prospects, Challenges, and Applications,” *IEEE Open Journal of Vehicular Technology*, vol. 3, pp. 278–320, May 2022, doi: 10.1109/OJVT.2022.3177946.
- [13] S. Wang and D. C. Ludoi, “A Capacitively-Coupled Single-Wire Earth-Return Power Tether for Aerial Platforms,” in *2022 IEEE Energy Conversion Congress and Exposition, ECCE 2022*, Institute of Electrical and Electronics Engineers Inc., Jun. 2024. doi: 10.1109/ECCE50734.2022.9948205.

- [14] X. Jin, X. Chen, C. Qi, and T. Li, "Investigation on the Electromagnetic Surface Waves for Single-Wire Power Transmission," *IEEE Transactions on Industrial Electronics*, vol. 70, no. 3, pp. 2497–2507, Mar. 2023, doi: 10.1109/TIE.2022.3170634.
- [15] M. Idrissi, M. Salami, and F. Annaz, "A Review of Quadrotor Unmanned Aerial Vehicles: Applications, Architectural Design and Control Algorithms", doi: 10.1007/s10846-021-01527-7/Published.
- [16] A. Balayan, R. Mallick, S. Dwivedi, S. Saxena, B. Haorongbam, and A. Sharma, "Optimal Design of Quadcopter Chassis Using Generative Design and Lightweight Materials to Advance Precision Agriculture," *Machines*, vol. 12, no. 3, Mar. 2024, doi: 10.3390/machines12030187.
- [17] A. Suarez, F. Real, V. M. Vega, G. Heredia, A. Rodriguez-Castano, and A. Ollero, "Compliant Bimanual Aerial Manipulation: Standard and Long Reach Configurations," *IEEE Access*, vol. 8, pp. 88844–88865, May 2020, doi: 10.1109/ACCESS.2020.2993101.
- [18] G. Malczyk, M. Brunner, E. Cuniato, M. Tognon, and R. Siegwart, "Multi-directional Interaction Force Control with an Aerial Manipulator Under External Disturbances," *Auton Robots*, vol. 47, no. 8, pp. 1325–1343, Dec. 2023, doi: 10.1007/s10514-023-10128-2.
- [19] M. N. Marques, S. A. Magalhães, F. N. Dos Santos, and H. S. Mendonça, "Tethered Unmanned Aerial Vehicles—A Systematic Review," Aug. 01, 2023, *Multidisciplinary Digital Publishing Institute (MDPI)*. doi: 10.3390/robotics12040117.
- [20] K. H. Chang and S. K. Hung, "Design and implementation of a tether-powered hexacopter for long endurance missions," *Applied Sciences (Switzerland)*, vol. 11, no. 24, Dec. 2021, doi: 10.3390/app112411887.
- [21] S. K. Phang, S. Z. Ahmed, and R. A. Hamid, *Design, Dynamics Modelling and Control of a H-Shape Multi-rotor System for Indoor Navigation*. IEEE, 2019.
- [22] K. C. Liao and J. H. Lu, "Using uav to detect solar module fault conditions of a solar power farm with ir and visual image analysis," *Applied Sciences (Switzerland)*, vol. 11, no. 4, pp. 1–21, Feb. 2021, doi: 10.3390/app11041835.
- [23] U. Pruthviraj, Y. Kashyap, E. Baxevanaki, and P. Kosmopoulos, "Solar Photovoltaic Hotspot Inspection Using Unmanned Aerial Vehicle Thermal Images at a Solar Field in South India," *Remote Sens (Basel)*, vol. 15, no. 7, Apr. 2023, doi: 10.3390/rs15071914.
- [24] D. K. Rajak, D. D. Pagar, P. L. Menezes, and E. Linul, "Fiber-reinforced polymer composites: Manufacturing, properties, and applications," Oct. 01, 2019, *MDPI AG*. doi: 10.3390/polym11101667.
- [25] K. Kumar Shaw, "Design and Development of a Drone for Spraying Pesticides, Fertilizers and Disinfectants." [Online]. Available: www.ijert.org
- [26] N. Sarode, P. Ghugal, S. Yadav, S. Dantule, and P. Nandankar, "A comprehensive review on solar panel cleaning robot technologies," in *AIP Conference Proceedings*, American Institute of Physics Inc., Apr. 2023. doi: 10.1063/5.0127800.
- [27] K. Zhao, Y. Lou, G. Peng, C. Liu, and H. Chang, "A Review of the Development and Research Status of Symmetrical Diaphragm Pumps," Nov. 01, 2023, *Multidisciplinary Digital Publishing Institute (MDPI)*. doi: 10.3390/sym15112091.

- [28] M. Ni *et al.*, “Design of Variable Spray System for Plant Protection UAV Based on CFD Simulation and Regression Analysis,” 2021, doi: 10.3390/s2102.
- [29] A. Jaswal and M. K. Sinha, “A Review on Solar Panel Cleaning Through Chemical Self-cleaning Method,” in *Lecture Notes in Mechanical Engineering*, Springer Science and Business Media Deutschland GmbH, 2021, pp. 835–844. doi: 10.1007/978-981-15-8542-5_73.
- [30] H. Aljaghoub, F. Abumadi, M. N. AlMallahi, K. Obaideen, and A. H. Alami, “Solar PV cleaning techniques contribute to Sustainable Development Goals (SDGs) using Multi-criteria decision-making (MCDM): Assessment and review,” *International Journal of Thermofluids*, vol. 16, Nov. 2022, doi: 10.1016/j.ijft.2022.100233.
- [31] S. Noorussbah, G. PB, S. Keerthivas, and P. E, “Aerial assessment of solar panel surfaces using drone,” vol. 56, no. ITM Web of Conferences, 2023.
- [32] S. A Patil, A. R Patil, V. N. Chougule, and S. T. Sanamdikar, “Design and Analysis of Automated Solar Panel Cleaning System,” *Current World Environment*, vol. 18, no. 3, pp. 1032–1045, Jan. 2024, doi: 10.12944/cwe.18.3.11.
- [33] C. Robert Quigley and P. W. Peter Chung, “Title of Thesis: DEVELOPMENTS IN CARBON FIBER ROD ANALYSIS FOR SPORTING GOODS APPLICATIONS.”
- [34] C. Geiger and S. Francisco, “The Real Costs of Institutional ‘Green’ Cleaning.” [Online]. Available: <https://www.researchgate.net/publication/228810874>
- [35] N. J. Lant, A. S. Hayward, M. M. D. Peththawadu, K. J. Sheridan, and J. R. Dean, “Microfiber release from real soiled consumer laundry and the impact of fabric care products and washing conditions,” *PLoS One*, vol. 15, no. 6, Jun. 2020, doi: 10.1371/journal.pone.0233332.
- [36] M. Mohandes, F. Schulze, S. Rehman, and W. Suliman, “Cleaning PhotoVoltaic Solar Panels by Drone Aerodynamic,” in *2021 4th International Symposium on Advanced Electrical and Communication Technologies, ISAECT 2021*, Institute of Electrical and Electronics Engineers Inc., 2021. doi: 10.1109/ISAECT53699.2021.9668543.
- [37] “Force_Control_of_a_Foldable_Robot_Arm_in_a_Drone_for_a_Solar_Panel_Cleaning_Task”.
- [38] T. Kim, B. Yu, C. Tirtawardhana, I. Made, A. Nahrendra, and H. Myung, *Development of Cleaning Module for Wall Climbing Drone with Bio-inspired Watering Mechanism*.
- [39] S. S. Sarkis *et al.*, “Novel Design of a Hybrid Drone System for Cleaning Solar Panels,” in *2022 Advances in Science and Engineering Technology International Conferences, ASET 2022*, Institute of Electrical and Electronics Engineers Inc., 2022. doi: 10.1109/ASET53988.2022.9735056.
- [40] *2019 6th International Conference on Signal Processing and Integrated Networks (SPIN): 7-8 March 2019, Amity School of Engineering and Technology, Noida, India*. IEEE, 2019.
- [41] K. M. Mishra, K. Babu M, S. C. U, and M. Nithya, “Drone Based Solar Panel Cleaning System,” in *2024 International Conference on Power, Energy, Control and Transmission Systems (ICPECTS)*, IEEE, Oct. 2024, pp. 1–5. doi: 10.1109/ICPECTS62210.2024.10780076.
- [42] A. F. B. M. Fisol, M. Zolkapli, and S. Shahbudin, “Design and Implementation of a Semi-Automatic Pesticide Spraying Quadcopter: Challenges and Opportunities,” in *2024 IEEE 22nd Student Conference on Research and Development, SCORED 2024*, Institute of Electrical and Electronics Engineers Inc., 2024, pp. 313–316. doi: 10.1109/SCORED64708.2024.10872632.

- [43] K. Baidya, A. J. R. Dampella, V. V. Surya Charan Paidipalli, S. Bansod, S. K. Singh, and P. Pal, "Pesticides Spraying Using Non-GPS-Based Autonomous Drone," in *2022 International Conference on Futuristic Technologies, INCOFT 2022*, Institute of Electrical and Electronics Engineers Inc., 2022. doi: 10.1109/INCOFT55651.2022.10094368.
- [44] J. T. Zou and V. G. Rajvee, "Drone-based solar panel inspection with 5G and AI Technologies," in *Proceedings of the 2022 8th International Conference on Applied System Innovation, ICASI 2022*, Institute of Electrical and Electronics Engineers Inc., 2022, pp. 174–178. doi: 10.1109/ICASI55125.2022.9774462.
- [45] N. Lionel, K. Bingi, R. Ibrahim, R. Korah, G. Kumar, and B. R. Prusty, "Autonomous Inspection of Solar Panels and Wind Turbines Using YOLOv8 with Quadrotor Drones," *Institute of Electrical and Electronics Engineers (IEEE)*, Sep. 2024, pp. 322–326. doi: 10.1109/icom61675.2024.10652395.
- [46] G. Terzoglou, M. Loufakis, P. Symeonidis, D. Ioannidis, and D. Tzovaras, "Employing deep learning framework for improving solar panel defects using drone imagery," in *International Conference on Digital Signal Processing, DSP*, Institute of Electrical and Electronics Engineers Inc., 2023. doi: 10.1109/DSP58604.2023.10167960.
- [47] N. Iversen, M. Birkved, and D. Cawthorne, "Value Sensitive Design and Environmental Impact Potential Assessment for Enhanced Sustainability in Unmanned Aerial Systems," in *International Symposium on Technology and Society, Proceedings*, Institute of Electrical and Electronics Engineers Inc., Nov. 2020, pp. 192–200. doi: 10.1109/ISTAS50296.2020.9462210.

Appendix – A

Here is the Arduino Nano Code for the servo sweeping mechanism.

```
#include <Servo.h>
Servo servo1; // First Servo
Servo servo2; // Second Servo (Opposite Direction)
const int pwmPin = 2; // D2 pin on Nano
const int buzzPin = 6; // D6 pin on Nano
void setup()
{
  servo1.attach(3); // Attach first servo to pin D2
  servo2.attach(4); // Attach second servo to pin D3
  center();
  pinMode(LED_BUILTIN, OUTPUT);
  pinMode(buzzPin, OUTPUT);
  // Wait for 5 seconds before starting motion
  for(int i = 0; i < 5; i++)
  {
    digitalWrite(LED_BUILTIN, HIGH);
    digitalWrite(buzzPin, HIGH);
    delay(100);
    digitalWrite(LED_BUILTIN, LOW);
    digitalWrite(buzzPin, LOW);
    delay(100);
  }
  digitalWrite(LED_BUILTIN, HIGH);
  digitalWrite(buzzPin, HIGH);
  delay(2000);
  digitalWrite(buzzPin, LOW);
}
void loop()
{
  unsigned long pwmValue = pulseIn(pwmPin, HIGH, 25000); // Timeout at 25 ms
  if (pwmValue > 1900)
  {
    sweep();
  }
  else if (pwmValue < 1000)
  {
    center();
  }
}
void sweep()
{ // Sweep both servos from 45° to 135° ( $\pm 45^\circ$  from center)
  for (int pos = 45; pos <= 135; pos++) {
    servo1.write(pos); // Normal motion
    servo2.write(180 - pos); // Inverted motion
    delay(10); // Increased delay to slow down (0.7x speed)
  }
  for (int pos = 135; pos >= 45; pos--) {
    servo1.write(pos);
    servo2.write(180 - pos);
    delay(10); // Increased delay to slow down (0.7x speed)
  }
}
void center()
{ // Move both servos to center (90°)
  servo1.write(90);
  servo2.write(90);
}
```

Appendix – B

Here are some of the parameter settings changed in the Pixhawk flight controller

Parameter	Value
Firmware	Copter stable v4.5.7
SYSIS_THISMAV	1
RTL_ALT	200
RTL_ALT_TYPE	1
FS_GCS_ENABLE	1
WP_YAW_BEHAVIOR	1
FS_THR_ENABLE	3
FS_THR_VALUE	945
FLTMODE1	9
FLTMODE3	5
FLTMODE6	0
FLTMODE_CH	6
INITIAL_MODE	9
FRAME_TYPE	1
LAND_REPOSITION	1
FS_EKF_ACTION	1
FS_CRASH_CHECK	1
FRAME_CLASS	9
BATT_MONITER	2
BATT_CAPACITY	6800
BATT_LOW_VOLT	19.8v
BATT_LOW_MAH	2000
BATT_FS_LOW_ACT	1
CAN_DI_PROTOCOL	1
CAN_PI_DRIVER	1
FENCE_ENABLE	0
GPS_TYPE	9

Table 13: Table showing Pixhawk 2.4.8 parameter tree values

Publication Details

Conference Name: 3rd International Conference on Data Science and Network Security (ICDSNS-2025).

Track Name: ICDSNS2025

Paper ID: 1383

Paper Title: Design and Development of an H-Frame Drone for Cleaning Solar Panels and High-Rise Buildings

Status: Submitted